2015

Thermo-Catalytic Methane Decomposition: A Review of State of the Art of Catalysts

Ahmed A. Ibrahim
King Saud University

Ahmed S. Al-Fatesh
King Saud University

Wasim Ullah Khan
King Saud University

Moustafa A. Soliman
The British University in Egypt, moustafa.aly@bue.edu.eg

Raja L. Al-Otaibi
King Abdulaziz City for Science and Technology

See next page for additional authors

Thermo-Catalytic Methane Decomposition: A Review of State of the Art of Catalysts

[1]Ahmed Aidid Ibrahim, [1]Ahmed Sadeq Al-Fatesh, [1]Wasim Ullah Khan*, [2]Mostafa Ali Soliman, [3]Raja Lafi AL Otaibi, [1]Anis Hamza Fakeeha
[1]*Chemical Engineering Department, College of Engineering, King Saud University, P.O. Box 800, Riyadh 11421, Saudi Arabia.*
[2]*Chemical Engineering Department, Faculty of Engineering, The British University in Egypt, El-Sherouk City, Egypt.*
[3]*King Abdulaziz City for Science and Technology, P.O. Box 6086, Riyadh, Saudi Arabia.*
wasimkhan49@gmail.com

(Received on 12th February 2015, accepted in revised form 6th June 2015)

Summary: The catalytic methane decomposition to produce carbon oxides–free hydrogen and carbon nanomaterial is a promising method feasible for larger production at a moderate cheap price. The produced hydrogen is refined and can be employed straight in fuel cell and in petrochemical industries to produce ammonia and methanol. Auto-thermal reforming of natural gas, partial oxidation, steam reforming are the conventional techniques for hydrogen production in industry, though these processes incur excessive costs for the purification of hydrogen from producing carbon oxides. Current research work on thermo-catalytic methane decomposition has concentrated on promoting the catalytic activity and stability for simultaneous production of pure hydrogen and elemental carbon. The carbon is generated as nanotubes, which are important for the use of this material in numerous new technologies. In the present review, thermodynamics of methane catalytic decomposition are elaborated and extensive considerations are given to the development of catalyst components by emphasizing the role of active particles, effect of catalyst promoters and support. The role of carbon catalyst in decomposing the methane catalytically, the morphology and characteristics of carbon produced and the catalyst deactivation is also discussed. The review also sheds light on the influence of operating parameters of temperature and space velocity. The performances of the frequently used catalysts are tabulated and types of reactors, influences of supports, promoters and preparation methods are outlined. Finally, the iron catalyst perspective towards hydrogen and carbon nanotubes productions by means of catalytic methane decomposition is presented in this work.

Keywords: Methane; Hydrogen; Carbon nanotubes; Iron; Dry reforming

Introduction

Sustainability and environmental impacts have been the two major challenges of the fossil fuel energy in the present era [1-3]. About 85% of the anthropogenic CO_2 emissions produced yearly is from fossil energy use [4]. The fast growth in the consumption of fossil fuels is an indicator for its end in the close future. Additionally, ever growing consumption of fossil fuels has caused environmental problems. Most of the fossil fuel products, CO_x, C_xH_y, NO_x, and SO_x might increase acid rain and global warming [5, 6]. Fig. 1 shows the historical production of fossil energy resources in million tons of oil equivalents (Mtoe) [7]. There is a strong need for the development of new technologies and methods for alternative energy sources. High cost and the under developing technology have been the main concerns of the other energy sources such as wind, solar, and biogas to be the replacement of conventional fossil fuels in the near future. Nuclear energy, another, alternating energy source raises a lot of safety concerns. Keeping all these things into consideration, there is consensus among governments, scientific communities and energy industries that fossil fuels will continue as a chief source of energy for predictable future, and the most likely approaches will comprise: (1) to decrease consumption of fossil fuels; (2) to advance renewable energy assets and skills; and (3) to monitor the undesirable environmental effects of fossil fuel utilizations [8, 9]. Hydrogen is presently seen as a halfway point as a promising energy route in both power generation and transport sectors. Water, the only combustion product of hydrogen makes it effective and versatile fuel. The chief benefits of hydrogen utilization as fuel is the substantial mitigation in greenhouse gas emission per unit of mechanical or electrical energy created from hydrogen which makes it the future clean fuel [10]. The other benefit of using hydrogen as a fuel is its higher efficiency in fuel cells compared to the usual

*To whom all correspondence should be addressed.

methods of electrical energy production from fossil fuels [11-13]. There is a huge potential for the utilization of hydrogen as a fuel in fuel cell for its usage in residential [14], commercial and industrial sectors [15]. But the method of production is one of the concerns for broader commercial scale production of hydrogen. Nowadays commercial production of hydrogen is largely centred on the processes of steam reforming and partial oxidation of hydrocarbons and carbonaceous feedstock, for instance, coal, natural gas, and petroleum fractions [16-22]. The hydrogen produced by methods, other than methane decomposition such as dry reforming and steam reforming, forms CO_x; which make severe problems for the further treatment of syngas. The purification of syngas contributes to increased cost and global warming as CO_2 is produced from CO in this process [23, 24]. At present steam reforming of methane constitutes 50% of world's hydrogen production. But to use it in fuel cell it should be CO_x free even a few ppm of CO is detrimental to low temperature fuel cell and a few ppm of CO_2 is toxic to alkaline fuel cells [25] and thus increase the cost of purification of hydrogen. The other ways of getting CO_x free hydrogen are water electrolysis and ammonia conversion. Electrolysis of water is a high cost process and there are several issues with the utilization of ammonia for the hydrogen production: (1) ammonia produced from hydrogen is not economically and environmentally feasible (2) ammonia gas pollutes the environment, with very unpleasant and harmful effects on human (3) ammonia itself, even at ppm levels, is poisonous to the catalyst of PEMFC [26]. On the other hand, another alternative of steam reforming, partial oxidation and water electrolysis and ammonia decomposition is the thermal/catalytic decomposition of methane [27-30]. The reaction comprises the methane molecule decomposition to produce hydrogen gas and solid carbon:

$$CH_4 \text{--------}> 2H_2 + C \qquad \Delta H^o = 75.6 \text{ kJ/mole} \qquad (1)$$

The required energy for a mole of hydrogen production in methane catalytic cracking and steam reforming is 37.8 kJ/mole and 63.3 kJ/mole respectively.

$$CH_4 + 2H_2O \text{------}> CO_2 + 4H_2 \quad \leftrightarrows^{\circ}_{298} = 253.2 \text{kJ/mole} \qquad (2)$$

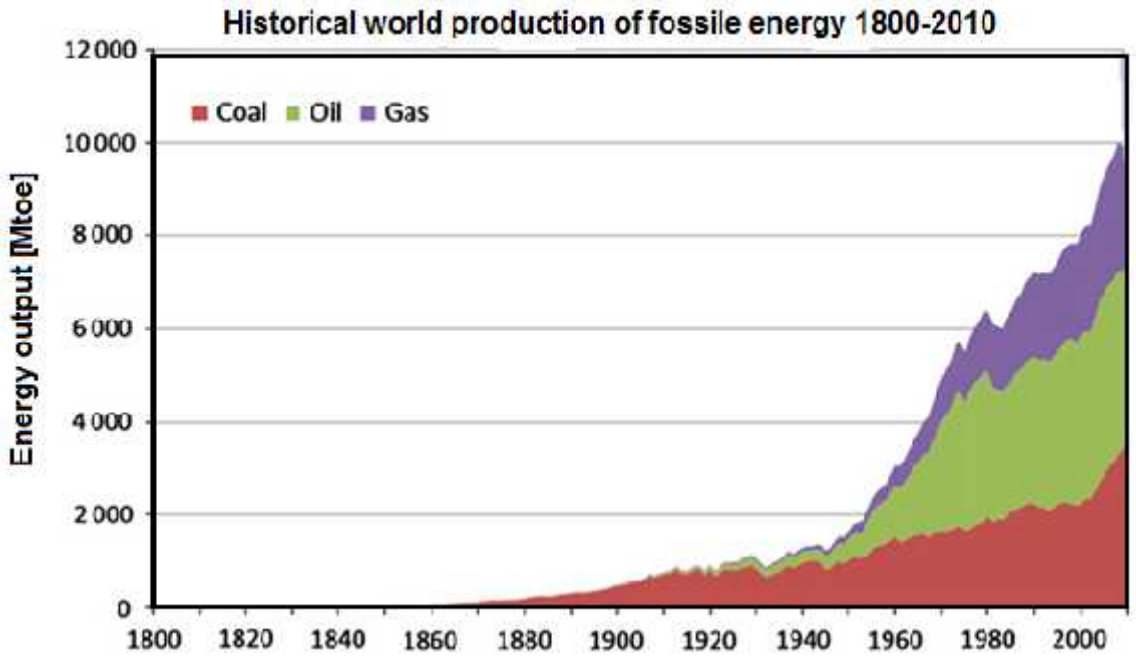

Fig. 1: Global production of fossil energy from1800 to 2010**.** Adapted from HÖÖK *et al*. [7].

The produced hydrogen is mixed with unreacted methane and can be separated easily by membrane separation or absorption. The separation process is less complex than the requirement for additional difficult separation processes that deal with carbon oxides. The production of pure hydrogen would be particularly important in fuel cell technology, as the Pt-based electrocatalyst is poisoned by CO. Reaction (1) eliminates the direct emission of CO_2 to the environment and the carbon produced in this reaction is considered as useful by-product which may have several commercial applications, and has a positive effect on process economy. The advantage of carbon produced depends on its type and properties [31, 32]. In this process, using different catalysts and different reaction conditions generates different carbon species such as, amorphous and graphitic carbon, carbon nanotubes, nanofibres and carbon allotropes as graphene structures [33]. Methane decomposition in the absence of catalyst requires a high amount of energy, *i.e*. 1200^0C for a practically good yield of hydrogen. The difficulty in direct methane conversion by catalytic and/or thermal processes is the strength of the methane C|H bond. The Gibbs free energy of methane is less than that of the products. The employment of catalyst significantly reduces reaction temperature, and also controls properties and type of co-products *i.e*. carbon species. There are three different types of catalysts for the methane decomposition (1) noble metals such as (Rh, Ru and Pt) [34], (2) metals from group VIII of transition elements [35-38] and (3) carbonaceous materials [39-42]. One of the main challenges accompanying with metal catalysts is the deactivation and recovery; the deposition of carbon formed covers the active sites during the reaction. The carbon formed in this reaction is one of the products, which means its production cannot be stopped. So reaction system and catalyst should be structured to retain good activity and stability despite the formation of substantial amounts of carbon.

Many reviews have been written on the subject with some of them concentrating on carbon nanotube production while others concentrating on hydrogen production. Chai *et al*. [43], discussed in their reviews the effect of metals, supports and temperature of decomposition, as well as the morphology of the carbon nanotubes produced and its growth mechanisms. Kumar and Ando [44] discussed the use of chemical vapor deposition to obtain carbon nanotubes (CNTs). They elaborated the growth mechanisms and its control. The CNTs have surprising properties: high electrical and thermal conductivity and many-times harder and stronger than diamond and steel respectively. It can be used as a structural material, catalyst, and catalyst support. It can also be used in carbon fuel cell as an anode electrode [44]. Li *et al*. [45] reviewed current development concerning the reaction mechanism and kinetics of group 8–10 base metal catalysts. Promoters, supports and preparation techniques are discussed. Abbas and Wan Daud [46] examined catalytic decomposition of methane using metal and carbon catalysts. They covered in their review topics such as the effect of operating conditions such as temperature and flow rate, at the rate of hydrogen production and the characteristics of the carbon produced, the types of reactors, operating conditions, deactivation and regeneration and the formation and utilization of the carbon produced. In addition to the topics discussed in the above reviews, Amin *et al*. [47] presented reaction thermodynamics, mechanism, kinetics, catalyst deactivation and regeneration as well as the use of fluidized beds in effecting the reaction. Ahmed *et al*. [48] reviewed a more general topic of non- catalytic and catalytic decomposition of hydrocarbons in which methane is a special case. In addition to the use of metallic catalysts, they included carbon as a catalyst and the use of plasmas to effect the decomposition. Abánades *et al*. [49] discussed industrial challenges for the different options for methane decomposition. They discussed non-catalytic, catalytic and the use of molten metals as a liquid medium to effect the reaction. Solid carbon can thus be skimmed off the surface of the molten metal. The same investigators continued the discussion of the challenges in another publication [50]. Lopez *et al*. [51] made a comparison between Ni, iron and carbon as a catalyst and found Ni-ex LDH-II as the most active. The least active catalysts in metals were catalysts based on iron. However, iron catalysts are resistant to deactivation. Carbon CB-v was the highest resistant catalyst against deactivation. However, carbon deposited on carbon catalysts is of low quality. Carbon nanotubes of high added value were produced using metal catalysts. This review will consider the through discussion of different features associated with methane catalytic cracking, sectioned into various parts; the first section elaborates the basics of the thermodynamics, advances in catalyst development and the role of catalyst and its deactivation. The second part comprises the operating conditions and morphology of carbon nanomaterial formation. The last part summarizes the performances of the frequently used catalysts in tabular form highlighting catalyst employed, types of reactors, preparation methods and conversion and the iron catalyst prospective.

Thermodynamics of Methane Decomposition

Thermal methane decomposition is a famous method that has been used for producing soot and hydrogen. Reaction (1) can be thermally conducted without a catalyst to attain highest hydrogen yield, however, higher reaction temperature is required (>1500 K) [52]. The thermodynamic data show that methane decomposition could be effected at moderate temperatures in the presence of appropriate catalysts. Hence the accomplishment of thermal decomposition of methane at reasonably low temperatures, the employment of catalysts is indispensable [53, 54]. Fig. 2 exhibits the equilibrium volume concentration of hydrogen in H_2 and CH_4 gaseous mixtures amounts to 94% [55, 56].

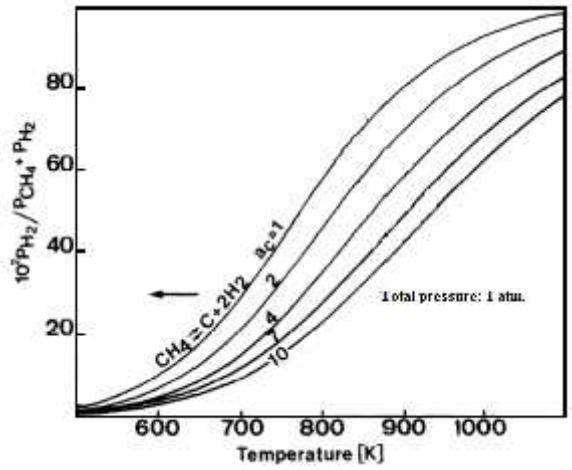

Fig. 2: Thermodynamic diagram showing isopotential curves for CH_4-H_2 gas mixtures [55].

In Fig. 2, a_C is the gas phase thermodynamic activity of carbon. Equation (3) states the definition of the thermodynamic carbon activity. The equilibrium constant in the process of cracking is commonly stated in terms of H_2 and CH_4 partial pressures [57-59]. The carbon activity is usually assumed one as shown in equation (4). Nevertheless, Fig.2 designates its impact on the equilibrium and the activity of the catalyst. Catalytic decomposition of methane encompasses the formation of solid carbon, such that the carbon atom dissociated from methane diffuses and reacts to form graphite layers.

$$a_C = P_{CH_4} / P_{H_2}^2 \times K_C \qquad (3)$$

$$K_c = \frac{P_{H_2}^2}{P_{CH_4}} \qquad (4)$$

It was observed that the carbon in the gas phase adsorbs on the active phase of the catalyst and diffuses through the catalyst as a result of existing diffusion driving force [60, 61]. The driving force for the bulk diffusion of carbon through the metal particle is attributed either to a concentration gradient or to a temperature gradient [62, 63]. Thermal reactions are commonly kinetically controlled and their products taken away from thermodynamic equilibrium while catalytic reactions are usually equilibrium controlled and their products near equilibrium. The overall reaction equilibrium constant which is a function of catalyst type can be stated in terms of hydrogen and methane partial pressures as [57]:

$$K_{eq} = \frac{\left(P_{H_2}^2\right)_{eq} C^S}{\left(P_{CH_4}\right)_{eq}} \qquad (5)$$

(Where C^S the carbon solubility in the active phase)

This equilibrium constant equation is for a gas phase in equilibrium with a solution of carbon in the active metal. The graphite solubility of particle differs from at the support. For instance, Yang *et al*. [64] accomplished carbon solubility in nickel in contact with a mixture of hydrogen and methane and obtained that the carbon quantity at saturation was 35% greater than for a mixture at equilibrium with graphite. The solubility of filamentous carbon is the equilibrium concentration of carbon dissolved in the active phase at the supporting side, which, determines the gas-phase composition at the coking threshold. Therefore, the threshold constant can be obtained from the formula:

$$K_m = \frac{P_{H_2}^2}{P_{CH_4}} \qquad (6)$$

The Gibbs energy of catalytic decomposition of methane changes in the temperature according to the following formula [65]:

$$\leftrightarrows G^0\,(\text{J/mole}) = 89658.88 - 102.27T - 0.00428T^2 - 2499358.99\,T^{-1} \qquad (7)$$

(Where T is temperature in Kelvin)

However, the expression provides approximate values since its derivation is based on graphitic carbon formation. In fact, the Gibbs free energy (Eq.7) demands values of temperatures above 819K for the formation of carbon. Nevertheless, many researchers obtained carbon formations below that temperature indicating the impreciseness of Eq. (7). Dent *et al*. exhibited that the gas-phase composition of systems forming carbon on transition metal catalysts differed considerably from the equilibrium values predicted for the reaction forming graphite (Eq.1). On the other hand, the study of Rostrup-Nielsen (57) on Ni based catalyst suggested that the Gibbs energy of catalytic decomposition of methane ($\leftrightarrows G^{cd}$) can be obtained by subtracting the expression for catalytic decomposition of methane that forms carbon deposit as graphite (Eq. 7) from the actual Gibbs free energy ($\leftrightarrows G^{a}$) of methane cracking.

$$\leftrightarrows G^{cd} = \leftrightarrows G^{a} - \leftrightarrows G^{0} \quad (8)$$

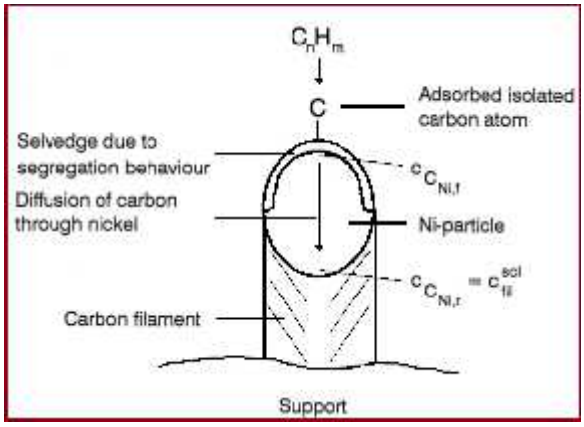

Fig. 3: Graphical representation of the mechanism of filamentous carbon formation [67].

The determination of rate constants in (Eq. 4) and Km (Eq.6) indicates that no cracking will take place ($K_c > K_m$) as K_m is measured at no gasification and at no carbon formation. When $K_c < K_m$, it is predicted that encapsulated carbon or carbon filaments are produced. A threshold constant K_{mf} for the formation of filamentous carbon on catalytic decomposition of methane was postulated by Zhang and Smith [66]. The constant has defined the value of K_c at which catalyst deactivation rate equals zero as a result of the filamentous carbon formation. Therefore, stable activity and formation of filamentous carbon in the methane decomposition over supported Ni and Co catalysts can be guaranteed by choosing K_m such that:

$$K_{mf} < K_c < K_m \quad (9)$$

Fig. 3 shows the graphical representation of the mechanism of filamentous carbon formation. While Fig. 4 exhibits the rate of carbon formation during methane cracking.

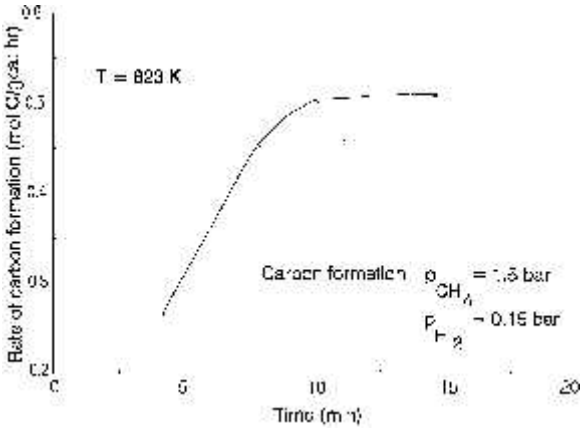

Fig. 4: Typical curve for rate against time in methane cracking [67].

Role of Active Metal

In this section, the discussion covers mainly different catalysts employed for catalytic decomposition of methane. The main function of the catalyst is to lower the operating reaction temperatures, which results by the reduction of the activation energy required for methane decomposition reaction. Since non-catalytic methane decomposition requires as high as 1200°C, the sluggishness of this reaction without catalyst employment leads to the fact that this reaction has no practical application at temperatures below 1000°C. However, catalytic methane decomposition can be carried out at temperatures as low as 500°C [68]. For instance, Ni/SiO_2 catalyst, being highly active for methane decomposition, presented optimal performance in the temperature range of 500-550°C [69]. Transition metals such as Ni, Co and Fe are known to be the most active for hydrocarbon decomposition. Among these transition metals, nickel has been recognized to have higher activity for the highly stable methane [70]. Co has the potential, as well, to be used as a catalyst for decomposition of methane, but there are some disadvantages associated with it such as less activity, toxicity issues, and higher cost. Additionally, Fe based catalysts have also been investigated for methane decomposition, but they showed lower activity as compared to Ni based catalysts [68]. Based upon the above discussion, comparison among above mentioned transition metals shows that the catalytic performance order is: Ni>Co>Fe [71].

The metal based catalysts have been extensively investigated as reported in the literature [72-80]. Pudukudy and Yaakob [72] studied the role of Ni, Co and Fe based monometallic catalysts for methane decomposition and inferred that Ni based catalyst was more active than Co and Fe based catalysts. Similarly, SBA-15 supported Ni, Co and Fe based bimetallic catalysts were investigated for hydrogen production and it was found that NiCo/SBA-15 was active while CoFe/SBA-15 was more stable than other catalysts [73]. Methane cracking at moderate temperature 550-600C was studied over Ni/Y zeolite catalysts and long term stability and carbon yield as high as 614.24 g_C/g_{Ni} was observed [74]. Fakeeha *et al*. [80] reported Ni-Co-Al catalysts for methane decomposition for the production of hydrogen and carbon nanofibers. They concluded that the catalyst containing 25wt% each of Ni and Co presented the best activity among the tested catalysts. The crystalline size of the Ni after reduction, in case of pure Ni based catalysts, was linked significantly to the catalytic activity of these catalysts for CH_4 decomposition reactions. Moreover, the highest carbon as well as H_2 yields was reported over the crystalline size of around 10.8 nm while relatively lower yields were reported in case of crystalline size of 20 nm and further increase in crystalline size to about 24 nm showed very low activity while crystalline size of 26 nm led to total deactivation. A novel catalyst based on Ni was investigated for CH_4 decomposition and carbon yields as high as 354–398 gC/gNi was reported before complete deactivation after 75 h showing maximum CH_4 conversion of about 10% [81].

Cai *et al*. [82] studied CH_4 decomposition over NiO nanoparticles for a reaction temperature of 300–500➡C. The advantage associated with the use of NiO after reduction without any support material was to operate the reaction at lower temperature. Prior to the requirement of carbon removal during 2–3 h, uniform CH_4 conversion of around 50% were observed. The carbon in the form of fibers or filaments was well lodged with un-supported NiO particles. The $NiCl_2$ based NiO having 7.5 nm particle size exhibited the best catalytic performance at 500➡C which was attributed to higher carbon deposition capacity *i.e*. C/Ni ratio. NiO particles generated from nickel nitrate with an average size of 9 nm showed an intermediate activity and stability. The nickel acetate based 10 nm sized NiO particles presented the lowest catalytic performance in terms of both activity and stability. Ni catalysts with high concentrations up to 90 wt.% were employed for the direct CH_4 decomposition for the production of H_2 and filamentous carbon [83]. However, lower CH_4 conversions were observed, *i.e*. at 500°C, 8% conversion was obtained, 15% at 550°C, and complete deactivation was observed at 600°C.

Rahman *et al*.[84] investigated 5-wt.% Ni/→-Al_2O_3 for CH_4 decomposition reaction using a thermo balance. They showed that faster deactivation was observed at 600–650°C due to faster carbon deposition rates. Moreover, use of lower catalyst weights (0.1–0.2 g) produced same results as well. Finally, they proposed a promising way to regenerate catalyst using partial gasification.

Awadallah *et al*. [27] studied the effectiveness of the combination of group VI (*i.e*. 25% each of Cr, Mo or W) and 25% Co supported over MgO for catalytic decomposition of methane to CO_x free hydrogen and carbon nanotubes. They revealed that group VI metal addition helped in improving catalyst surface properties due to inducing stronger interaction with the support *i.e*. MgO and CoO_x crystals. Additionally, they attributed the longer catalytic stability to the higher dispersion and stabilization of Co particles via formation of $CoMO_4$ and $CoWO_4$ species.

Lua *et al*. [85] investigated Ni-Cu-Co alloy particles for hydrogen production via (catalytic decomposition of methane) CDM. They showed that Ni-Cu-Co alloy catalysts, with different atomic compositions and crystalline sizes ranging from 12.6 to 15.9 nm presented good catalytic activities for 650 to 775 °C. Co addition to Ni-Cu alloy inhibited the quasi-liquid phenomenon, thus catalyst stability, enhanced at higher temperatures, but further increase in Co contents resulted in phase separation.

Wang and his co-workers [86] tested sol-gel based active and stable Ni–Fe–SiO_2 catalysts for the direct decomposition of undiluted methane to produce hydrogen and carbon filaments at 823 K and 923 K. They indicated that the Ni–Fe–SiO_2 catalysts retained activity for a longer time than that of Ni–SiO_2 catalyst at higher reaction temperature, *i.e*. 923 K, while at a lower temperature the same catalyst showed a reverse trend. They attributed this catalytic behavior to iron atoms that entered into the Ni lattice forming Ni–Fe alloy.

Venugopal *et al*. [87] studied the performance of a Ni/SiO_2 catalyst with nickel loadings in the 5-90% range in a fixed-bed reactor. The results revealed that initially increase in nickel loading affected catalytic activity and stability positively up to 30% Ni loading. However, further

increase in Ni loading resulted in poor catalytic performance.

Suelves *et al*. [88] used Ni based commercial catalyst and reported that hydrogen concentration was around 80% at a temperature of 700°C. He added that the value of conversion attained corresponded to the theoretical equilibrium value. Ogihara *et al*. [89] investigated M/Al_2O_3 (M=Fe, Co, Ni and Pd) and Pd-based alloys containing Ni, Co, Rh or Fe. They concluded that Fe, Co and Ni/Al_2O_3 catalysts deactivated quickly at 700°C, while Pd/Al_2O_3 catalyst showed the initial methane conversion of 15% which gradually decreased to <15% after 270 min. The Pd-alloy based catalysts presented high activity and stability above 700°C, especially, $Pd–Ni/Al_2O_3$ and $Pd–Co/Al_2O_3$ produced the highest hydrogen yields.

Co-doped Al_2O_3 catalysts having porous structures and high surface areas were tested for methane decomposition. The catalytic activity and stability results showed that the prepared catalysts were reported to be active and stable, and this performance was related to catalyst characteristic properties as well as the operating conditions used for decomposition reaction. In addition, the increase in methane conversion was observed with respect to feed (N_2:CH_4) ratio, metal loading and reaction temperature [90].

Jana *et al*. [91] studied the behavior of cobalt catalysts, for hydrogen production via decomposition of methane, prepared by different precipitating agents including sodium carbonate, ammonium hydroxide and urea. They revealed that precipitating agent employed influenced physicochemical properties of the catalysts which, in turn, affected catalytic performance. The results indicated that Na_2CO_3 or $CO(NH_2)_2$ based catalysts remained significantly active even at lower temperatures. Smaller metal particle size and lower degree of aggregation were the main factors influencing metallic Co catalytic performance. Moreover, the urea based Co catalyst produced the highest H_2 at 600°C for over 12 h time on stream while the catalyst prepared by Na_2CO_3 exhibited notable activity even at a temperature as low as 400°C.

Cobalt based catalysts having 48 wt% Co supported over MgO were investigated for the production of carbon via methane decomposition at a reaction temperature of 900°C as a function of the calcination temperature T_c [92]. Transmission electron microscopy results for carbon produced showed that carbon presented three structural forms, including shapeless tangles, shell-like materials, and carbon filaments. Temperature-programmed reduction (TPR) and X-ray diffraction (XRD) results revealed that the calcination temperature at 700°C ($T_c \leq 700$°C) generated Co_3O_4, Co_2MgO_4, and (Co, Mg)O (solid solution of CoO and MgO); at T_c=800°C, Co_3O_4 and (Co, Mg)O were located while only (Co, Mg)O was identified for T_c=900°C. Furthermore, the filamentous carbon formation was well favored by the metal particles which were originated from the reduction of the solid solution.

Jana *et al*. [93] studied methane decomposition for the production of hydrogen using urea precipitation based cobalt catalysts. After drying, calcination of the prepared catalyst changed it to metal oxide. Moreover, use of different reducing environment converted metal oxide to actual metallic cobalt catalyst. The results indicated that catalytic activity and deposited carbon type were fairly influenced by the reduction ambience. In addition to reduction ambience, catalyst pre-treatment had a strong influence in the H_2 production as well. Thermal treatment of the catalyst using nitrogen as pre-treatment gas presented the best catalytic activity. The better performance for nitrogen atmosphere was associated with smaller size of Co nanoparticles (*i.e*. higher surface area) in the bulk in comparison to the other two pre-treatment atmospheres used. The results also showed that the possible product, in addition to hydrogen, generated from Co based catalyst was graphene and this was observed when reducing gas employed was methane.

Piao *et al*. [94] investigated the performance of cobalt aerogel catalyst supported over alumina, prepared by sol-gel and supercritical drying method, for catalytic methane decomposition. The characterization and activity results as well as the effect of calcination and reaction temperature showed that the $CoAl_2O_4$ spinel structure was formed in the calcined catalyst. Increase in cobalt loading increased the quantity of the nanotubes deposited over catalyst surface and higher rate of reaction was observed with increased reaction temperature which led to faster catalyst deactivation. The deposited carbon nanotubes were having smooth walls and uniform diameter distribution.

Cobalt based catalysts were employed in catalytic decomposition of methane with reaction temperature in the range of 475–600°C and pressure nearly 1 bar. The findings inferred that influencing factors for the process included a catalyst method of preparation, support material nature and temperature regimes and 60–75 wt% Co catalysts supported over alumina and prepared by co-precipitation showed the

best catalytic performance at reaction temperature of 500°C. Characterization techniques such as XRD, EXAFS and TEM indicated that the results were close to previously investigate Co and Ni catalysts. However, as compared to Ni catalysts, Co catalysts generated hollow-like core morphology carbon filaments [95].

Co based catalysts supported over SiO_2 with metal loading varying from 5 to 30 wt.% were investigated for CH_4 decomposition reaction [96]. In addition, the effect of different parameters, such as metal (Co) dispersion, reaction temperature and introducing CO or H_2 in the feed, on the kinetics of CH_4 decomposition was reported as well. The results indicated that decreasing Co dispersion from 13% to 5% increased initial catalytic activity and decreased catalyst deactivation rate. Since increased reaction temperature led to more carbon deposition, thus the deactivation rate increased with increasing reaction temperature. The study of CH_x migration from the metal to the support presented the fact that the formation of filamentous carbon played important role in carbon removal from the metal surface and thus contributing to the catalyst stability during CH_4 decomposition reaction. Moreover, addition of H_2 or CO to the feed decreased carbon formation rate and carbon removal rate increased because of increased carbon diffusion through the Co.

Abdullahi *et al*. [97] reported methane decomposition over Fe-MgO catalyst for the selective production of single-walled carbon nanotubes (SWCNTs) having narrow chirality and diameter distribution. They employed different characterization techniques to clarify the structure and chemical state of the species which contributed to SWCNT growth as well as reaction selectivity, SWCNT chirality and diameter distribution, purification protocols effectiveness and carbon yield were characterized by High resolution electron microscopy, Raman and optical absorption spectroscopy, temperature programmed oxidation, energy dispersive X-ray spectroscopy and nitrogen physisorption. Effect of reaction temperature studied implied that carbon increased with an increase in temperature, although above the optimum reaction temperature, SWCNTs' selectivity decreased. The results indicated that catalyst selectivity towards SWCNT growth was well affected by the iron oxide dispersion degree inside the support *i.e*. MgO.

Fe based catalysts were tested in a fixed bed reactor for the production of hydrogen and filamentous carbon via methane decomposition [98]. The results indicated that catalyst performance was well affected by the addition of textural promoter as well as Mo as a dopant. Al_2O_3 based Fe catalyst presented slightly better catalytic performance than that of catalysts based on MgO. On the contrary Mo addition to Al_2O_3 based catalysts showed poor performance while improved performance was observed for Mo doped MgO based catalysts. Additionally, the effect of different parameters, such as catalyst reduction temperature, the reaction temperature and the space velocity, showed that at temperatures higher than 800°C Fe based catalysts yielded higher methane conversion with filamentous carbon having interesting properties. Moreover, the formation of multiwall carbon nanotubes was observed at temperatures higher than 700°C.

Tang *et al*. [99] investigated the catalytic performance of ceria supported iron catalysts (Fe–CeO_2) for the production of hydrogen by methane decomposition. The Fe–CeO_2 catalysts exhibited better activity than the catalysts based on iron alone. The catalyst containing 60 wt.% Fe_2O_3 and 40 wt.% CeO_2 presented optimal catalytic activity as well as the highest iron metal surface area. The better metal dispersion helped in maintaining the active surface area for the reaction. Reaction temperature increase from 600➡C to 650➡C increased methane conversion. The formation of high mobility lattice oxygen in the solid solution within the vicinity of catalyst helped in the oxidation of carbonaceous species resulting in continuous CO trace amount formation. This oxidation could help in a longer catalyst lifetime as it minimized catalyst deactivation caused by carbon deposition. Additionally, the formation of filamentous carbon also helped to extend the catalyst life.

Effect of Support

Conversion of methane depends upon the catalyst matrix which comprises the active material and the support [87, 100]. In this section the role of support on the catalytic performance for methane decomposition will be discussed in detail. The support material affects the conversion and the researchers have been reported that unsupported catalysts are less active than the supported catalysts. For example, Li *et al*. [101] prepared two samples with and without support using co-precipitation method. They reported that unsupported NiO was not active under study conditions while Ni supported over Al_2O_3 showed good activity and stability for the same reaction conditions. In a similar way, Toebes and co-workers [102] found negligible carbon nano fibers over an unsupported Ni catalyst for methane decomposition. However, unsupported Ni catalyst presented very stable and active performance for C_2H_4 decomposition which they associated with

higher activity demand for CH_4 dissociation than C_2H_4 decomposition.

The interaction between active metal and support plays a vital role in catalytic activity of the catalyst. Echegoyen and his co-workers [103] showed that methane conversion increased with a decrease in the interaction between the active component and the support. Additionally, the surface area and electronic state of metal influenced methane activity as well. For instance, the study of Ni catalyst supported over magnesia and silica concluded that the formation of solid solution between Ni and Mg lowered methane conversion while the higher methane conversion, in case of silica, was attributed to the possible formation of unstable nickel silicates which, at higher temperature during reduction, might decompose [68]. Ermakova and Ermakov [70] studied Ni/SiO_2 and Fe/SiO_2 and showed that silicate free Ni catalyst presented the maximum yield (384 g C/g Ni) while the yield decreased to 40 g C/g Ni when 1.5 to 2% of the nickel was converted to nickel silicate. In case of Fe, silica addition, depending upon silica loading, decreased or increased methane conversion. Takenaka, along with his team mates, [104] investigated nickel catalyst supported over different supports (SiO_2, TiO_2, graphite, Al_2O_3, MgO and SiO_2-MgO) calcined at 600°C for 5 h. In addition, they employed X-ray diffraction to characterize the catalysts. The results concluded that methane conversion increased for the catalyst which had lower metal to support interaction even with the equivalent surface area. At the end, among all tested supports for the same operating conditions, silica and titania supports showed the highest methane conversions.

Among different important factors affecting methane conversion, the structure of the support material and its textural properties e.g. porosity also influence methane conversion. Ermakova *et al*. [68] investigated nickel based catalysts having different support promoters *i.e*. silica, magnesia, alumina, and zirconia. They inferred that the pore structure of the catalyst significantly affected its catalytic performance and stability. Moreover, using silica as promoter instead of support, highest methane conversion with longer catalyst lifetime was observed and this performance was associated with the higher pore width for silica promoted nickel catalyst. The outlet gas composition and deposited carbon morphology could also be affected by the support structure. For instance, the high oxygen capacity supports such as ceria could produce oxides of carbon e.g. carbon monoxide unless surface oxygen of the catalyst made to be immobilized so as to prevent the reaction between oxygen and deposited carbon [105].

Takenaka along with his team workers [106] studied Co based catalysts supported over different supports, including MgO, Al_2O_3, SiO_2 and TiO_2 and showed that using MgO and Al_2O_3 as support for Co metal catalysts resulted in higher activity as compared to the rest of the supports investigated. Additionally, they came across the fact that better catalytic performance in case of Co/Al_2O_3 and Co/MgO was due to smaller particle sizes of active metal. Moreover, they showed that carbon nano fibers grew with more ease for Co particle diameters of 10–30 nm while Co particle diameters more than 30 nm presented no activity. Finally, characterization techniques including K-edge XANES and EXAFS, confirmed the presence of Co in the form of metal during the reaction irrespective of catalyst support type and reaction temperature. Temperature programmed catalytic reaction technique was used to study the catalytic performance of the supported Ni catalyst. The results revealed that the onset temperature of methane decomposition reaction got influenced by the nature of the supports employed [107].

Hu and Ruckenstein [108] suggested that nickel particles with very small size were obtained when the solid solution of NiO and MgO was reduced. This concept was reconfirmed recently in the work of Gac *et al*. [100]. They proved that the high initial decomposition rate was attained by using catalyst having small nickel crystallite strongly interacting with magnesia. Ismagilov *et al*. [109] investigated silica glass fiber supported Ni catalyst for the growth of carbon nano fibers via methane decomposition reaction. They employed washcoat and ion exchange methods to prepare catalysts and found that carbon nano fibers having diameter 20–50 nm and carbon capacity as high as ca.55 g C/g Ni were produced for washcoat based catalyst. Recently, catalysts with structure based supports, such as Perovskite structured oxides, have been used for decomposition reaction [110–113]. Smaller metal particles with stronger metal support interaction enhanced catalytic activity and carbon formation with improved structure. The reduction of $LaFeO_3$ produced Fe nanoparticles, which, in turn, generated single wall carbon nano tubes (SWCNTs) with diameters in the narrow range of 0.8–1.8nm [114]. The factor responsible for SWCNTs growth was uniform and close distribution of Fe fine nanoparticles over $LaFeO_{3-x}$. Chen *et al*. [110] inferred that good activity and carbon yield was attained with $Ni–Co/La_2O_3$ catalyst employed, without any pre-treatment, in decomposition reaction. Kuras *et al*. [111] reported better stability at higher temperature for perovskite precursor based Ni

catalyst. They also showed that Ni particle size was not much affected by the reduction and the reaction temperatures. Self-combustion preparation method was employed to prepare $LaNiO_3$ type perovskite which was subsequently tested for methane decomposition at reaction temperature of 873 and 973 K [112]. The excellent activity results showed that catalyst used for the simultaneous production of carbon nanotubes (CNTs) and hydrogen remained stable even after 22 h of reaction at 973 K. The main reason behind the stable catalytic performance of Ni catalyst originated from $LaNiO_3$ precursor's activation was the high degree of metal crystallites dispersion over La_2O_3 matrix [113]. The higher metal dispersion degree helped in controlling the metal particle sintering as well. In addition, La_2O_3, being textural promoter or support, increased the BET surface area and also exhibited as an electronic promoter [115, 116]. The addition of La_2O_3 to Raney Fe improved activity and stability of the catalyst.

In addition to metal oxides, carbon based materials such as nano fibers have been reported as support for methane decomposition reaction catalysts. Since carbon nano fibers possess a mesoporous structure with high surface area varying from 100–300 m^2/g, these fibers are a good choice for decomposition reaction catalyst system [117]. Carbon nano fibers, produced from methane decomposition over Ni, Ni–Cu, Ni–Fe, Co and Fe–Co supported on alumina, were used as support for Ni catalysts [118–120]. The secondary carbon (carbon produced from methane decomposition over carbon supported Ni catalyst) yield remained 224 g/g Ni over Ni/CNF (Ni–Cu) catalyst and 268.5 g/g Ni on Ni/CNF (Ni–Fe) catalyst, respectively. Zeolites have also been reported to be the support for decomposition reaction catalysts [120–124]. Ashok *et al*. [120] tested different supports such as HY, USY, SiO_2 and SBA-15 to estimate their catalytic performance for Ni based catalyst. The catalyst comprising 30 wt.% of Ni supported on HY exhibited the best activity and stability. The performance was ascribed to the acidic nature of the support as well as the Ni metal particle size. Guevara *et al*. [122] employed surfactant-assisted method to prepare mesoporous Ce-MCM-41 for Ni based catalysts and showed that the catalyst presented a very stable performance in the decomposition reaction.

Ni based catalyst supported on ZSM-5 was utilized to produce MWCNTs in the lower temperature range of 673–823 K [123]. The decomposition reaction was found to take place mainly in the zeolite channels at 673 K as suggested in TEM characterization images. However, at temperature over 673 K, the formation of carbon on the catalyst surface was observed as well. Jehng and his research fellows [124] investigated the performance of Ni/MCM-41 catalyst. They discussed the MWCNTs' deposition on catalyst surface and suggested tip-growth mechanism for the formation of MWCNTs in which catalyst particles detached from support is found at the tips of the CNTs formed. Choudhary *et al*. [125, 126] investigated the effect of support on the carbon formed and CO evolved during methane decomposition. They found that both carbon morphology and CO produced were well influenced by the support. No filamentous carbon formed over Ni/H-ZSM-5 catalyst in the temperature range of 723–873 K, while Ni/HY and Ni/SiO_2 catalysts produced filamentous carbon in tested temperature range (723–873 K).

The ability to improve metal support interaction and active metal dispersion has attracted the researchers to employ CeO_2 as support in methane decomposition reaction. Li *et al*. [105] investigated Ni/CeO_2 catalysts and reported the effect of different preparation methods as well. Tang *et al*. [99] employed Fe supported over CeO_2 was used in decomposition reaction and the results indicated that the catalyst containing 60 wt.% Fe_2O_3 on 40 wt.% CeO_2 exhibited the best catalytic performance. However, the product stream showed CO_x detection, which was attributed to the lattice oxygen, originating from CeO_2, reaction with deposited carbon. Odier *et al*. [127] reported improved H_2 production by using Pt/CeO_2 catalyst. They suggested that the spillover of noble metal's carbonyls towards partially reduced CeO_2 hydroxyl groups was the main reason behind improved catalytic performance. Moreover, the reverse spillover of lattice oxygen towards active metal helped in gasifying deposited carbon which was confirmed with CO_x detection in the product stream.

Different support materials such as Al_2O_3, MgO, or SiO_2, has been used as catalyst surfaces with high dispersion for (Single walled carbon nanotubes) SWCNT growth [35–38]. MgO has been more attractive than that of SiO_2 and Al_2O_3. MgO-supported catalysts may be a better choice because of their efficiency for SWCNT and (Double walled carbon nanotubes) DWCNT growth as well as ease of MgO separation from the carbon product through acid leaching without any loss or damage to carbon structure, while in case of SiO_2 or Al_2O_3, it is very difficult to remove these support materials from carbon product. Li *et al*. [132] investigated SWCNTs growth via chemical vapor deposition over porous MgO support based on thermal decomposition of its salts ($Mg(NO_3)_2$ and $MgCO_3$) and showed that MgO presented excellent results. Ning and his team [133]

reported formation of a uniform $MgFe_2O_4$/MgO solid solution structure as a result of calcination at 1173 K for 12 h and concluded that the reduced structure facilitated several active sites, having a diameter around 4 nm, which helped in generating SWCNTs and DWCNTs. Hydrothermal treatment was applied to produce porous and lamella-like Fe catalysts supported over MgO which became a simple approach for high yield of DWCNTs [134]. The hydrothermal treatment method was also found promising in preparing hydrophilic oxides supported metal catalysts. Ethanol-thermal treatment was employed to prepare a porous MgO supported Fe catalyst [135]. The resulting catalyst having pores in the range of (50 nm to 5 μm) was used to produce SWCNTs with a quality better than that of originating from the previously reported catalysts. Direct growth of SWCNTs on a flat support surface, e.g. SiO_2/Si wafer, has also been reported to be applied in the micro-electronics or nano-scale research on physic-chemical properties [136]. In another study, Wang *et al*. [137] used chemical reduction with microwave irradiation to produce Fe/Ru and Fe/Pt based bimetallic catalysts supported over the SiO_2 flat surface. Li *et al*. [138] utilized carbonyl complexes decomposition to prepare Fe–Mo nanoparticles with sizes ranging from 3 to 14 nm via different protective agents. These nanoparticles were subsequently precipitated from propanol and redispersed in n-heptane. SWCNTs were grown by dropping or spin coating the solution onto Al_2O_3/Si or SiO_2/Si substrates. Kong *et al*. [139] reported individual SWCNT production over silicon wafers having a micro level well defined pattern of catalytic material. The CNTS generated were perfect with individual CNTs having 1–3nm diameter and up to tens of micron length.

Role of Carbon Catalysts

Catalyst plays a significant role in generating methane thermal decomposition and determining its performance. The adaptability of carbon as a catalyst was recognized a long time ago [140]. In recent years, carbon material has become a hot research area, and carbon-based catalysts are developing rapidly [141-144]. Generally, two different types of catalyst have been developed for thermo-catalytic methane reforming; they comprise metal and carbonaceous catalysts [46]. Carbon based materials are considered as ideal catalysts due to desirable features such as low material cost, high surface area and thermal stability [145-148]. Moreover, they offer certain advantages over metal catalysts due to tolerance to sulfur and other potentially harmful impurities in the feedstock [148]. In addition, the carbon based catalyst can be easily separated from reaction system, which is very convenient for recovery and reuse. Different kinds of carbon materials have been developed for methane catalytic decomposition. These include carbon black, glassy carbon, activated carbon (AC), diamond powder, graphite, fullerene, carbon nanotubes and acetylene carbon [142, 148-150]. The factors influencing the performance of a catalyst include the number of active sites available for reaction, reactant chemisorption capacity and capability to form surface intermediates having suitable strength [151]. Indeed, most of the previous studies have shown that the activity of carbon catalysts relates to their structural and textural surface properties [41].

Abanades *et al*. [152] investigated the solar thermo-catalytic decomposition of methane employing carbon black catalysts for the production of pure hydrogen in a packed-bed reactor. Solar power supplied the requied heat to derive endothermic reaction. The rate of the heterogeneous decomposition reaction was improved by carbon particles. Several operating parameters such as temperature and residence time of the feed gas through the catalyst bed were were tested to measure the performance of thermochemical properties of the reactors. The parameters affected the chemical conversion and hydrogen yield. Indeed, A very high methane conversion to hydrogen was attained with negligible side products. Nevertheless, gradual catalyst deactivation was seen due to carbon formation on the surface, with acetylene as the chief developing by-product.

Rechnia *et al* [153] reported the suitability of carbon catalyst for the methane decomposition to generate hydrogen. In their study, they tested the addition of methanol as a promoter that generates potentially active carbonaceous deposits for suppressing the catalyst deactivation. Activated carbon gained from the hazelnut shells was tested at different reaction temperatures. The use of the ethanol lengthwise the methane boosted the yield of hydrogen produced and maintained at a high level the catalyst activity.

Muradov *et al*. [148] studied the carbon materials and in particular the role of carbons during decomposition reaction which is related to the relation between their surface and structural properties. The concentration of active sites over the surface is the governing factor affecting the activity of the carbons. Moreover, the activation energy of methnae decomposition reaction over carbon based catalysts is estimated to be in between the activation energy of the decomposition reaction over transition metal based catalysts and activation energy of

methane decomposition without using catalyst (non-catalytic).

Serrano *et al*. [154] studied a range of carbon materials which include ordered black carbons, carbon nanotubes, mesoporous carbons, activated carbon, graphite and coke as catalyst for thermo-catalytic methane decomposition to produce hydrogen. They investigated the activities of different carbon materials by means of temperature programmed conditions. No conclusive correlations were observed for minimum temperature for activation of the process and parameters such as crystallinity, surface area, and the oxygenated groups concentration. Nevertheless, a decreasing linear relationship has been found to exist between the minimum activating temperature and the proportion of defects in the graphene layers. Thus, carbon materials having a high defect concentration, such as an ordered and interconnected mesoporosity, followed by activated carbon or carbon blacks, show higher activity. Alternatively, highly ordered carbon catalysts exhibit little activity. Al-Hassani *et al*. reported the production of hydrogen via catalytic methane decomposition using as catalyst two different types of activated carbon [42]. Rates of ethane decomposition at 820, 860, 900, and 940°C were conducted. The Pore structure of the catalyst was observed to have negligible effect on the initial rate of decomposition, but had a significant effect on the time required for full catalyst deactivation. Higher temperatures increased rate of decomposition of methane and decreased the deactivation time. The mesopores activated carbon catalysts showed high resistance to catalyst deactivation, whereas the micropores ones resulted in fast and complete catalyst deactivation.

Lee *et al*. [155] studied methane decomposition at high temperatures ranging from 1,293-1,443 K using carbon black catalyst. Nearly total methane conversion and stable condition for two and half hours' time on stream was attained at 1,443 K, and the activation energy of the catalytic reaction over carbon black was 198 kJ/mol. In addition, it was observed that the specific surface area decreased as the amount of deposited carbon increased. Fig. 1 Global production of fossil energy from1800 to 2010, Microporuos activated carbon catalyst was used for production of hydrogen from decomposition of methane [156]. No appreciable catalytic activity effect of surface area was observed, but as the surface area and the pore volumes increased, the resistance of the catalysts to deactivation increased. Carbonaceous deposit formed during the reaction block the micropores and hence was responsible for the catalyst deactivation.

Guil-Lopez *et al*. made comparative examination in terms of initial activity and stability of methane decomposition via metal based catalysts (Ni and Fe) and carbon based catalysts (activated carbon , carbon black, carbon nanotubes and graphite) [157]. They found that activity of carbon catalysts was similar to that of the non-pre-reduced metal catalysts and the carbon black were shown to be the most resistant catalyst against deactivation. Table-1 displays the principal catalytic parameters of metal catalysts for methane decomposition while Table-2 presents the literature summary for carbon catalysts in the thermo-catalytic decomposition of methane. Abbas and Wan Daud studied the apparent kinetics of methane decomposition and the deactivation kinetics of activated carbon catalyst using various reactant residence times in the temperature range of 775–850°C in a fixed bed reactor [46]. The authors' apparent kinetics gave the reaction order of 2 and activation energy of 163 KJ/mol instead of 0.5 as reported by other investigators and deactivation order of 0.5 and the deactivation energy of approximately 177 KJ mol/ [53, 158, 159]. In an earlier work, the investigators studied the catalyst deactivation kinetic due to carbon deposition with time and found that the catalyst activity decreased almost linearly with the amount of carbon deposited at 800°C, while the substantial diffusion effect took place at higher temperatures [46]. Methane decomposition over carbon catalyst was investigated kinetically and the apparent reaction order was found to be 0.5 for both activated and carbon black -based catalysts [53,158, 159]. Hence, the rate equation for carbon-catalyzed decomposition of methane can be expressed as follows:

$$-r_{CH_4} = k\, p_{CH_4}^{0.5} \qquad (10)$$

Considerable work has been carried out in the catalytic methane decomposition using metal catalysts like Ni, Fe Co and carbon materials. Customarily metal exhibit higher catalytic activities and the need for a lower reaction temperature than carbon catalysts, however the carbon catalysts reveal their own benefits. It is expected for catalysts to lose the activity with time on the stream because of the constant carbon formation during catalytic methane decomposition. Lately, attractive topic research is developed in the area of catalytic methane decomposition using carbon materials, like activated carbon, as the support for metal catalyst. The utilization of carbon-assisted catalysts provides certain advantages over metal catalysts.

Table-1: Review summary of metal catalytic decomposition of methane.

Catalyst constituents	Method of forming catalyst	Reactor type	Operating conditions	Product/ conversion	Ref.
La_2O_3 doped Ni and Ni–Cu Raney-type promoter amount 0.03- 0.06 g	30Ni-50Cu leaching out the aluminium with a concentrated NaOH solution	tubular reactor	Activ.=600°C T=400–900 °C.	nanofibers and multiwall carbon nanotubes 79%CH_4 conversion 22hr	[166]
75%Ni–12%Cu/Al_2O_3, 70%Ni–10%Cu–10%Fe/Al_2O_3	mechanochemical activation	rotating flow reactor	Enhanced T=700–750 °C 600–650 °C.	Nanofibers Carbon Y= 150–160 g/g. HY>70	[167]
Mo doped Fe/Al_2O_3 or Fe/MgO	Fusion	fixed-bed reactor	T=800-900°C	filamentous carbon, at=900°C 87%CH_4 conversion &93%v of H_2-Conc. Space velocity =1L/g/h	[89]
Ni–Cu–Al 78/6/16 ratio	co-precipitation vs fusing of the metallic nitrates	fluidized bed		60 l /hf hydrogen and 15 g/ h carbon nanofibers	[168]
cobalt acetate in ethylene glycol	cobalt acetate in ethylene glycol PPt. agents: sodium carbonate, ammonium hydroxide urea.	TG/DSC thermobalance	T=400-1000°C	T=high, ammonia. T=low carbonate	[82]
Fe-based catalysts doped with Mo/Al_2O_3 or MgO	fusion method	a thermobalance	Maximum performance of Fe-Mo catalysts 700-900	Methane (70%) MWCNTs (5.3 g/h).	[169]
Ni/SiO_2	incipient wetness impregnation	fixed-bed quartz micro reactor		15 wt.% Ni/SiO2 At 650C Fully regenerated filamentous carbon	[170]
Ni metal foam wash-coated with SiO_2	wet impregnation	quartz tube reactor	T=550-750➡C	MWCNTs Optimum 20% wt Ni at 650➡C	[171]
Fe/ HZSM-5 zeolite, HBETA zeolite, and porous precipitated Al_2O_3	microwave assisted Impregnation method.	quartz tube	T=800➡C	H_2 10–30 vol% CNT	[162]
Ni–Mo and Co–Mo/ Al_2O_3	Commercial	fixed bed horizontal reactor	T=700➡C	Ni–Mo catalyst (CNTs) Co–Mo catalyst (Amorphous carbon).	[172]
Nickel–copper based catalysts textural promotes with SiO_2, $Al2O_3$, TiO2, MgO	Fusion method	fluidized bed reactor	T=700➡C For 7h	CNTFs	[173]
NiO-M/SiO_2 (where M=AgO, CoO, CuO, FeO, MnO, and MoO	impregnation method	fixed-bed reactor	T= 700 °C	8:2 ratio NiO/SiO_2 promoted with CuO give the highest hydrogen yield	[174]
Ni, Ni:Cu, Fe or Fe:Mo / Al_2O_3 or MgO		rotary bed reactor	700 °C for the Ni-based catalysts and 800 °C for the Fe-based catalysts. Space velocity of 12 Ndm^3 $CH4\cdot(h\cdot g\ cat)^{1}$ for Ni-based catalysts and 1.5 Ndm^3 $CH4\cdot(h\cdot g\ cat)^{1}$ For Fe-based catalysts.	H_2 -yields 14.4 $Ndm^3H_2\cdot(h\cdot g$ cat)-1Initial CH_4 conversion of 82% 3hr reaction Carbon nanofilament	[30]
Ni/Al_2O_3 Ni-Cu/ MgO Fe/Al_2O_3 Fe-Mo/ MgO	fusion method	rotary bed reactor	700°C for the Ni-based catalysts and 800°C for the Fe-based ones Space velocity 2 Nl CH_4 (h g $cat)^{-1}$	Carbon nanofilaments	[175]

Table-2: Literature summary for carbon catalysts in the thermo-catalytic decomposition of methane.

Catalyst[a]	T[b]	VHSV/(L/hgcat)		XCH_4[c]	Carbon deposits	td	Ref.
	(°C)	Total	CH_4	(%)	(g/gcat)	(h)	
AC-micro (AC)	950	504	50.4	-	0.13	1.42	[146]
AC-meso (AC)	950	1115	111.5	-	0.34	1.42	[146]
CG (AC)	850	0.6	0.6	51	0.45	8	[133]
SUPRA (AC)	850	0.6	0.6	32	0.35	8	[133]
GAC (AC)	850	0.6	0.6	25	0.40	8	[133]
CMK-5 (OMC)	950	545-2000	54.5-200	-	~8	24	[41]
CMK-5 (OMC)	1000	400-3000	40-300	1.5-3.5	~20	48	[176]
CB-bp (CB)	1100	1911	191.1	-	5.0	3	[146]
CB-v (CB)	1100	1361	136.1	-	8.5	4	[146]
DCC-N103(p) (CB)	850	15	15	13	-	2	[177]
DCC-N220(p) (CB)	850	15	15	7	-	2	[177]
XC72 (CB)	900	100	100	-	2.74	20	[178]
BP2000 (CB)	900	100	100	-	6.13	20	[178]
RC (AC)	850	15	15	19	>4.32	>5	[140]
CC (AC)	850	15	15	21	2.45	5	[140]
AlRC (AC)	850	15	15	61	>36	>10	[140]
SiRC (AC)	850	15	15	26	>4.90	>5	[140]
BP2000 (CB)	850	15	15	12	1.31	5	[140]

a: Carbon catalyst, with the type marked in the parentheses. AC, OMC and CB means activated carbon, ordered mesoporous carbon and carbon black, respectively
b: Reaction temperature
c: Maximum methane conversion on the catalyst
d: Deactivated time of the catalyst

Jin *et al* [194] investigated catalytic methane decomposition for hydrogen production employing Fe-Al_2O_3 supported over activated carbon catalysts. Their characterization results displayed the straight reduction of ferric nitrate upon carbon support to metallic iron at 870 ➡C. The effect of Fe/Al_2O_3 weight ratio was shown to influence the textural properties and catalytic methane decomposition. In addition, Fe and Al_2O_3 loading decreased the surface area and pore volume of the catalyst. Mesopores formation of catalyst enhanced the catalytic activity and stability.

Zhang *et al*. [160] studied the catalytic methane decomposition for hydrogen production, using Ni doped carbons obtained from raw coal and direct coal liquefaction residue. Their results exhibited that that the Ni doped carbon performed better stability and activity at 850➡C reaction temperature when compared to corresponding metal and carbon catalysts. Moreover, the procedure for preparing Ni doped carbons influenced the reducibility of the carbon composition. Simialrly, the catalytic activity was affected by the amount and the morphology of the formed carbon.

Justyna Majewska, Beata Michalkiewicz synthesized cobalt nanowires in one-step method of carbon nanotubes via methane decomposition at the temperature of 400 °C and 800 °C, using Co/ZSM-5 catalyst [161]. The outcome of investigation demonstrated the easy generation of cobalt-filled carbon nanotubes. A better quality carbon can be produced at 800 °C reaction temperature as evidenced by the characterization techniques.

Operating Conditions

The catalytic decomposition of methane into carbon oxides–free hydrogen and carbon is viable method of reforming. The potentiality of the useful carbon co-product rests on its characteristics, which depends on the process and conditions used. Carbon can be used in the production of fibers, plastics, composites, metal carbides and metal–carbon composites. The value of the carbon formed in the catalytic methane decomposition depends on the operation conditions and the type of catalyst used. Reactors used include fixed and fluidized beds. Fixed bed reactors could suffer from reactor plugging due to the growth of carbon on the catalyst surface. Fluidized bed reactors and rotary bed reactors show promise for continuous operation whereby carbon can be separated in cyclones. Catalyst regeneration is carried out using air or steam. Employment of metal-based catalysts generates high-quality forms of carbon that compensate the cost of the catalyst. The work of Suelves *et al*. [88] investigated commercial catalyst based on Ni for catalytic decomposition of methane for CO_2-free hydrogen production employing different operating conditions. They have stated that operating conditions dictate the time for catalyst deactivation *i.e*., a shorter lifetime of the catalyst was observed when higher temperature and methane flow were used. Fig. 5 shows the reaction temperature effect in which increase in temperature leads to increased methane conversion and hydrogen production. Similarly Fig. 6 exhibits the dependence of CH_4 conversion and hydrogen production on catalyst amount.

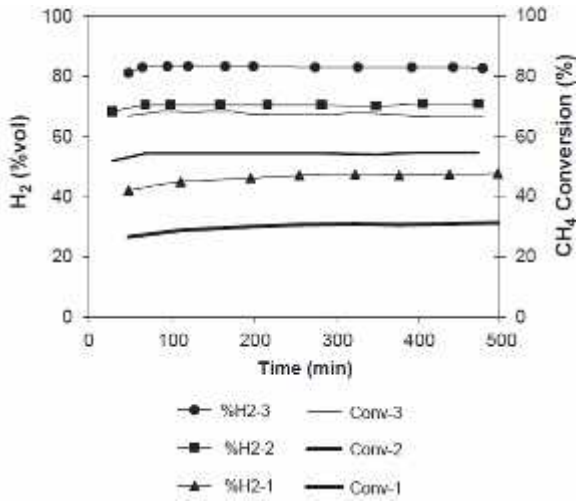

Fig. 5: Hydrogen production and CH_4 conversion versus reaction temperature.

Run 1: 550°C; run 2: 650°C; run 3: 700°C. Amount of catalyst: 2 g; Flow: 20 ml/min.

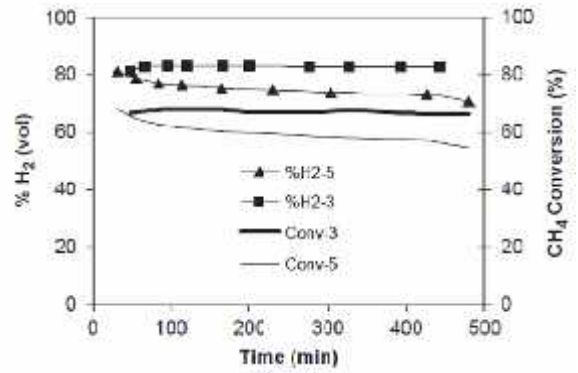

Fig. 6: Effect of catalyst amounts on production of hydrogen and CH_4 conversion.
Run 3= 2 g; run 5= 0.3 g. T= 700 ◦C; Flow = 20 ml/min.

Nuernberg *et al*. [90] examined the effect of operating conditions for thermo-catalytic decomposition of methane using Co/Al_2O_3 catalyst. They found that the catalytic performance is well affected by characteristics of the catalyst as well as the operating conditions used. The increase in methane conversion was observed with respect to molar ratio (N_2:CH_4), reaction temperature and metal loading. The best conditions for hydrogen production included 20 wt% loading of Co, molar ratio of 6:1 and 800°C reaction temperature. Fig. 7 displays the catalyst activities in dealing with different N_2:CH_4 molar ratios. The results inferred that increase in a molar ratio increased average methane conversion. When the amount of the inert gas was very high in the feed, the catalyst gave the highest conversion value (22%). Alternatively, the increase in methane concentration in the feed *i.e*., employing N_2:CH_4 molar ratios of 2.5:1; 1:9 and 4.5:1, lowered the conversion values. The lesser amount of catalyst active sites may be responsible for this effect.

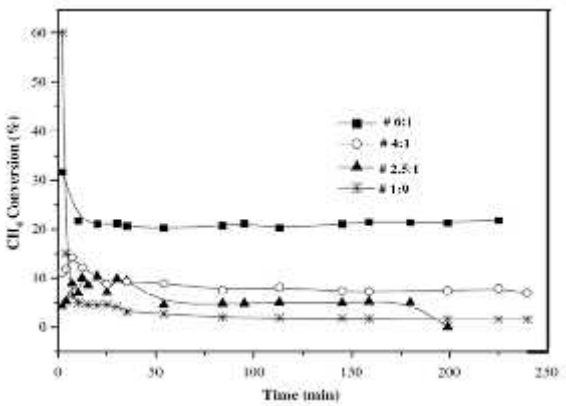

Fig. 7: Methane decomposition over 9-Co/Al_2O_3 catalysts. Performance of the 9-Co/Al_2O_3 catalyst in the CH_4 conversion with time-on-stream at 700 °C at different N_2:CH_4 molar ratios.

The laboratory scale bubbling fluidized bed reactor was used to investigate →-alumina baed copper catalyst for thermo-catalytic decomposition of methane [162]. The influence of different operating parameters including reaction temperature, contact time, total flow rate and CH_4 inlet concentration was studied. From Fig. 8, it can be seen that shorter deactivation times with lower methane conversions (even lower than equilibrium conversions) were observed when higher concentrations of methane were employed. This may be ascribed to the intrinsic kinetics of decomposition reaction, *i.e*., more carbon deposition leads to lower activity with respect to reaction time. Nonetheless, lower methane conversion is observed and this conversion does not drop directly to zero.

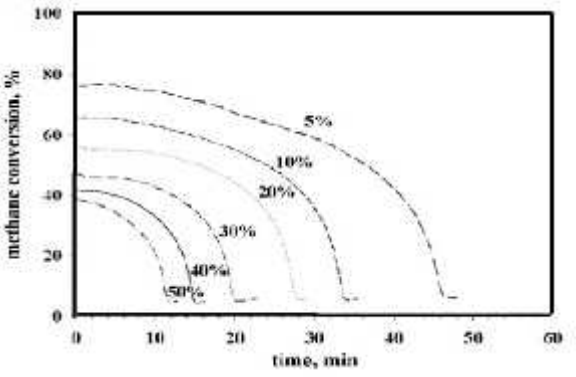

Fig. 8: Influence of methane concentration on methane conversion at T=800°C; mcat =25g; Q= 45Nl/h.

The deposited carbon perhaps plays a role in the catalytic activity [163]. In Fig. 9, it can be seen from carbon formation rate curves that rapid growth reaching its maximum is observed in the initial period. After that a decline from maximum takes place which leads to a residual constant value. The methane concentration affects the carbon formation rate in that increase in methane concentration increases carbon formation. It can be concluded that, depending upon operating conditions employed, type as well as the amount of carbon formed contribute to catalyst deactivation [65, 88,164].

Catalyst Deactivation

The employment of a catalyst facilitates the reaction to take place at lower temperatures much below the required value of 1200°C. The catalyst activity decreases over time. The catalytic activity and/or selectivity loss over time is an extreme difficult and a continuing problem in the course of catalytic reactions. The variation of the activity due to deactivation is concisely reported [165].

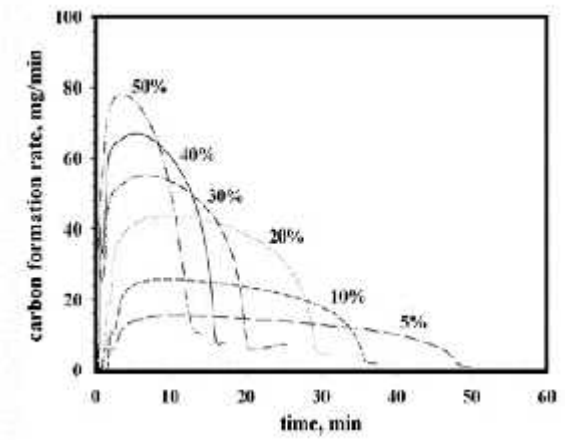

Fig. 9: Influence of methane concentration on carbon formation rate at T=800°C; mcat =25g; Q= 45Nl/h.

The activity of a catalyst at any time may be expressed as

$$a = \frac{-r_A'}{-r_{A_0}'}$$

$$= \frac{\text{rate at which reactant A is converted by the catalyst}}{\text{rate of reaction of A using a fresh catalyst}} \quad (11)$$

While the rate at which the catalyst deactivates may be written as

$$-\frac{da}{dt} = k_d . C_i^m . a^d \quad (12)$$

where k_d is the deactivation rate constant, d the order of deactivation, m measures the concentration dependency.

In the catalytic methane decomposition using carbon catalysts, the kinetic profiles of methane decomposition over activated carbon and carbon black catalysts display fast catalytic activity initially, followed by a fairly mild drop in methane decomposition rates. Due to carbon deposition, loss of the catalyst surface deactivated the catalyst [159]. Catalyst deactivation, which is mainly due to surface area reduction and pore obstruction arising from carbonaceous deposits from methane decomposition reaction, is responsible for the loss of catalytic activity. Probably, the total rate of CH_4 decomposition is the combination of carbon nucleation rate and carbon crystalline growth rate. In the activated carbon catalysts, the blockage of the pore mouths by carbonaceous deposits significantly reduces the micro pore volume and BET surface area and thus the loss of catalytic activity prevails [166]. The catalytic activity of deposited carbon is less than that of the original carbon and hence methane conversion has decreased with time [144]. Fig. 10 shows the surface area and total pore volume versus reaction time for methane decomposition using carbon black catalyst. In the case of metal catalysts, gas-side of the metal surface is covered by excess carbon. Encapsulating carbon decreases the available metal surface area for methane cracking to take place. Moreover, the reduction of the active surface area brings about reduction of heat input to the metal which in turn diminishes the carbon solubility and its diffusion through the metal and consequently, the rate of carbon encapsulation escalates [61]. Suelves *et al.* [88] investigated the catalytic methane decomposition in a fixed bed reactor at different operating conditions employing a commercial Ni-based catalyst to obtain pure hydrogen. They investigated the mechanism of catalyst deactivation, and obtained hydrogen concentration of about 80% at 700°C, which is close to the thermodynamic values. It has been displayed that operating conditions influence the time for catalyst deactivation. Higher temperature and higher methane flowrate reduce the catalyst life. In Fact, using 700°C reaction temperature and space-time of 1 s, the catalyst activity was maintained over 8 h in the stream. On the contrary, the catalyst became deactivated after 90 min using 0.2 s space-time while the amount of carbon deposited was reduced to half.

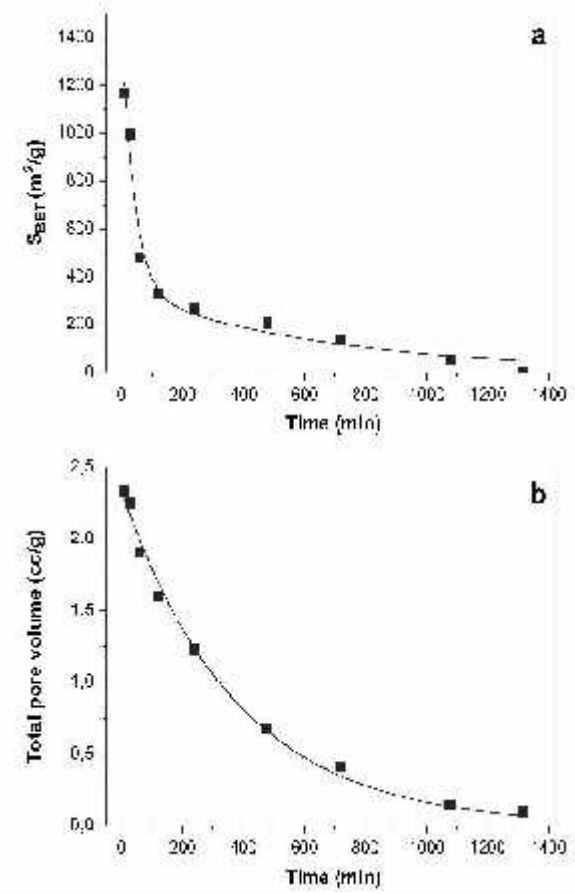

Fig. 10: Variation of the BET area (a) and total pore volume (b) against reaction time at T=950°C and GHSV=360 h^{-1} [154].

Morphology and Characteristics of Carbon Formed

Hydrogen and different carbon nanomaterial are produced from the catalytic methane decomposition depending on the type of catalyst and reaction conditions used. The carbon products include carbon nanotubes (CNTs), carbon fibers (CFs), carbon blacks (CBs), and carbon flakes [168-173]. There is a strong relationship between the morphology of the formed carbon and its performance. For instance, for CNTs, the open end has prospective applications in heterogeneous catalysis as the inner surface of the tubes avails room for reactant molecules and also form irregular and varying configurations due to their sharp ends and dangling bonds when used in the emission devices, whereas the CNTs require pretreatment to take away the cap in the case of close end [174]. Li *et al*. [175] performed methane catalytic decomposition in a tubular using porous supported iron catalyst such as zeolite HZSM-5, zeolite HBETA and precipitated Al_2O_3. They found CNTs with different morphologies. The CNTs formed on zeolites were short and had close ends and catalyst particles did settle on the CNTs tips. While with zeolite HBETA, CNTs formed on HZSM-5 showed more turns and discontinuities. Moreover, complex CNTs with various morphs and a wide range of size were grown on precipitated Al_2O_3; In fact, catalyst particles rested at the CNTs tips. Their study of CNTs on zeolites and Al_2O_3 revealed two different growth mechanisms for similar reaction conditions, which are the tip growth mode for Al_2O_3 and the base growth mode for zeolites. Fig. 11 depicts the morphology of carbon products. Saraswat and Pant investigated thermal catalytic methane decomposition using a nano-size Ni-Cu-Zn/MCM-22 catalyst [176]. Their result indicated the formation of CNTs which looks like interlaced nano filaments emerging from nickel particles over catalysts. Fig. 12 displays the morphology of carbon formed via SEM Characterization.

Cunha *et al*. [177] studied the effectiveness of Ni–Cu alloyed Raney-type catalysts for the hydrogen production via catalytic methane decomposition. They found different structures of carbon were formed due to the different active phases. The SEM micrographs of the Ni30Cu50 obviously display lengthy carbon nanofibers (CNF) after decomposition reaction at 600°C. Fig. 13 presents a TEM picture, displaying filaments with narrow hollow cores.

Pinilla *et al*. [30] investigated Ni and Fe-based catalysts for catalytic methane decomposition. Their results exhibited the carbon nano filaments formation of the order of 12–14 $gC \cdot g_{cat}^{-1}$ for the Ni-based catalysts and 1.5–2.3 $gC \cdot g_{cat}^{-1}$ for the Fe-based catalysts. In Fig. 14, Ni-based catalysts generated fishbone-like carbon nanofibres whereas Fe-based catalysts produced chain-like carbon nanofibres.

Zhang *et al*. [178] studied catalytic methane decomposition employing Ni/MgO and Ni/O-D catalysts. Their results revealed that catalyst kinds and reaction conditions influenced not only the methane conversion, but also microcosmic morphology of carbon.

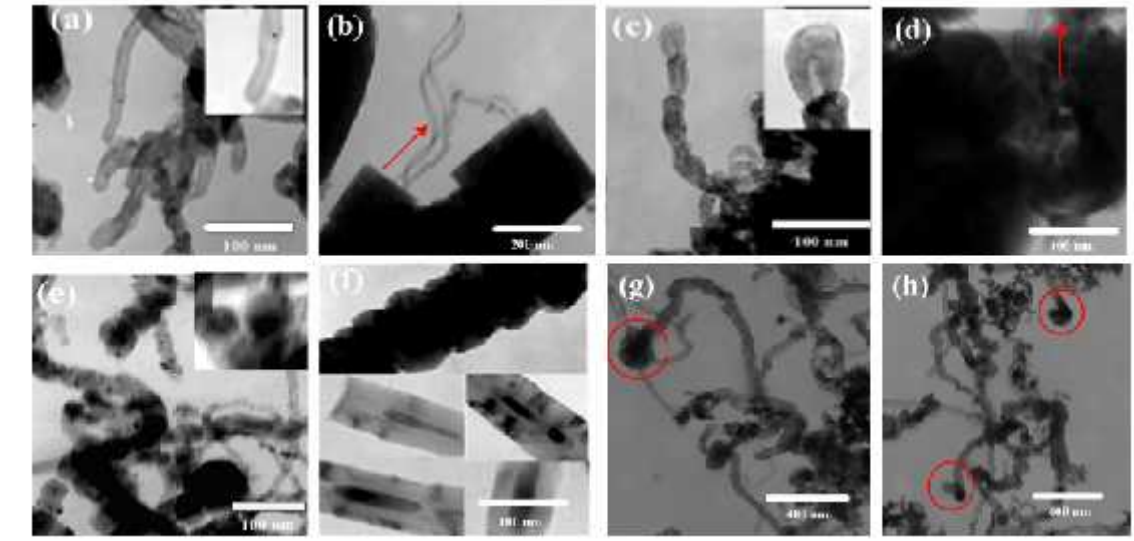

Fig. 11: Morphologies of carbon products over (a and b): HBETA zeolite; (c and d): HZSM-5 zeolite; (e–h): Al_2O_3 (TEM graphs) [162].

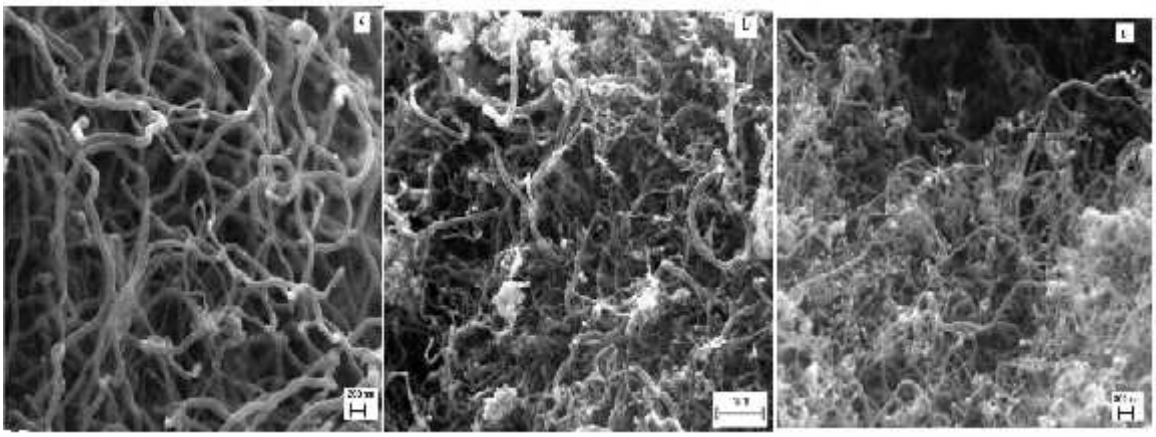

Fig. 12: SEM micrographs of as grown CNTs over the catalyst (a) catalyst 50%Ni-10%Cu-10%Zn/MCM-22 (b) catalyst 50%Ni-15%Cu-5%Zn/MCM-22, and (c) catalyst 50%Ni-15% Cu-15%Zn/MCM-22 after a CDM run at 750°C [163].

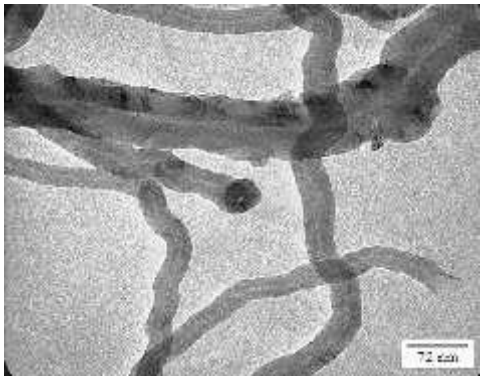

Fig. 13**:** TEM micrograph of the carbon deposit obtained on Ni30Cu50 at 600 °C [164].

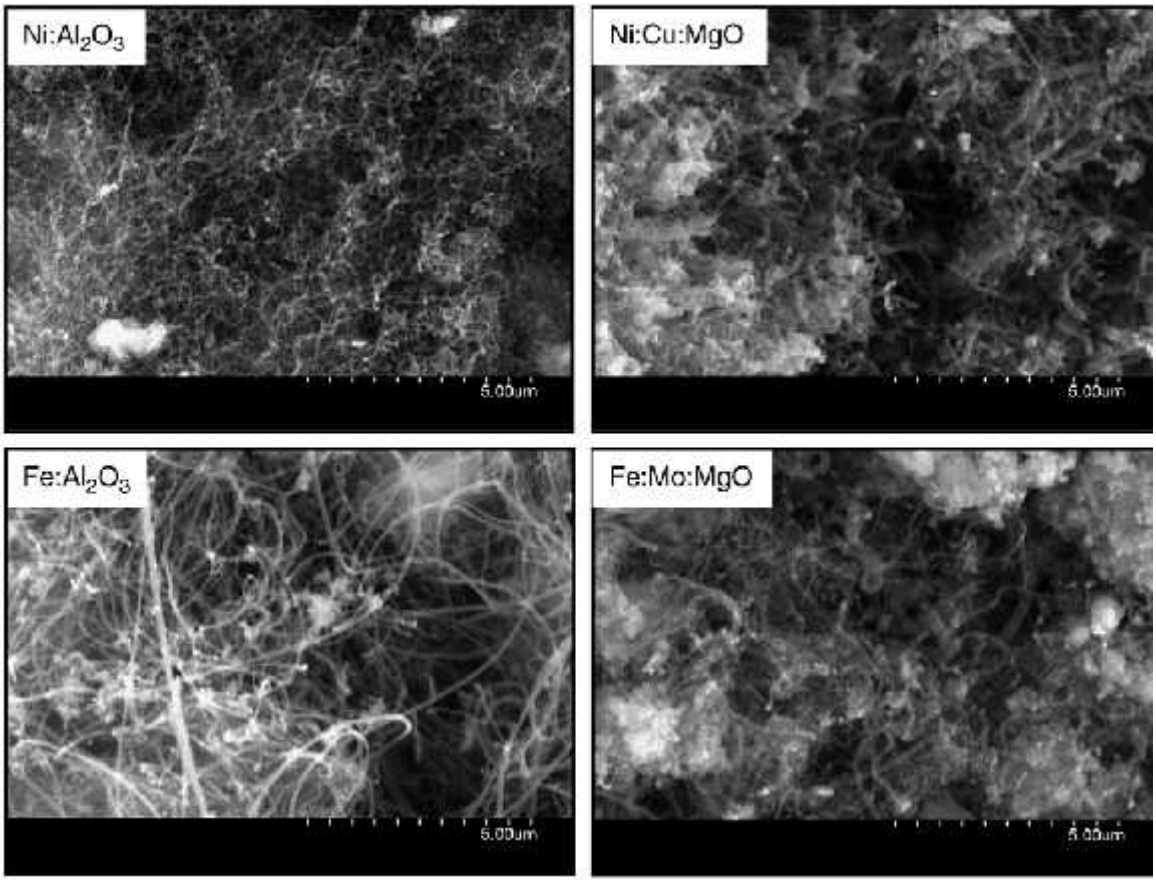

Fig. 14**:** SEM micrographs of the carbon nanostructures formed by CMD with each catalyst [30].

Catalysts based on iron

A huge interest has been granted to the development of iron-based catalysts for their cheaper, non-toxic properties than Ni catalysts. Indeed, iron-based catalysts are one of the least expensive catalysts used for the thermo-catalytic methane decomposition. Muradov studied thermo-catalytic decomposition of methane over an iron oxide catalyst [54]. The author concluded that the catalytic activity of iron catalyst was high at temperatures above 600°C and the yield was near equilibrium values at 800°C. The alumina supported iron catalysts were explored by Shah *et al.* [192] at a temperature range of 400-1200°C. First, they studied pure iron catalysts and concluded that their effectiveness decreased with decreasing reactor temperatures. Better activity was obtained using binary molybdenum- iron catalysts and binary palladium-iron catalyst. The authors also investigated the effects of temperature on hydrogen production and found that, above 800°C production decreased with most of the active catalysts, likely due to the thermal deactivation of the catalyst. Although Fe-based catalyst has lower catalytic activity than Ni-based one at a low reaction temperature [193] it is likely to find higher methane conversion on Fe catalyst at high temperatures (above 700°C), because high temperature enhances the methane decomposition reaction equilibrium and making use of the catalytic activity of AC itself as the catalysts. A comparison between Ni and Fe based catalysts were performed by Pinilla *et al*. [30] in a rotary reactor. Although Ni-based catalysts are more active at a given temperature, the use of iron-based catalysts allows for the use of higher temperature and thus obtains methane conversion above 80 %. The type of nano-carbon obtained is different. The use of Al_2O_3 as a support gives better results than MgO. Pinilla *et al*. [98] studied the addition of Mo as a promoter to Fe-based catalyst. It improves the performance if MgO is used as a support and there is a little effect if Al_2O_3 is used. Methane Conversion up to 87% is obtained if the temperature is increased to 900°C. Tang *et al*. [99] tested the use of ceria as a support giving improved performance. Optimal catalytic activity was obtained for a catalyst of composition 60 wt% Fe_2O_3 + 40 wt % CeO_2. Reshetenko *et al*. [195] studied the effect of adding Ni or Co to Fe-based

catalysts from 600 to a 650°C reaction temperature. The investigators concluded that the temperature range was effective for methane decomposition. The best performance was for a catalyst of the composition, 50–65 wt.% Fe, 5–10 wt.% Co (or Ni) and 25–40 wt.% Al_2O_3. Torres *et al*. [182] found that the addition of Mo to Fe based catalysts led to the increase of the rate and amount of deposited carbon. Chesnokov and Chichkan found that by adding Fe to Ni-Cu/ Al_2O_3 catalyst, it was possible to increase the reaction temperature from 700 to a 750°C and thus increase the conversion [180]. Cunha *et al*. [177] found that the addition of Cu to Raney type iron catalyst improves catalyst performance. Takenaka *et al*. [196] found that Al_2O_3 is a better support than SiO_2 for Fe catalysts. Konieczny *et al*. [197] studied preparation methodology for Fe based catalysts. Avdeeva *et al*.[71] examined catalyst preparation effects on the amount of filamentous carbon produced. Fe-Co- Al_2O_3 catalysts gave the most effective carbon formation. Ermakova *et al*. [198] investigated the reaction temperature effect of the Fe-based catalyst. They used a temperature range of 650-800°C. They found that temperature should be higher than 680°C for the catalyst to be stable and to operate for a long period of time. Oliveira *et al*. [199] found that Sn hinders methane decomposition in chemical vapor deposition reaction to produce carbon. Wang *et al*. [86] found that Ni-Fe-SiO_2 has a better performance than Ni-SiO_2 when the reaction temperature is 650°C. The reverse happens when reaction temperature is 550° C. Yamaguchi *et al*. [200] suggested using a cycle in which methane decomposition is carried out in one step. Steam is used in the second step to remove carbon deposited. The catalyst is iron based. The simultaneous addition of CeO_2 and ZrO_2 improved catalyst activity and stability. Polymer-based composites were prepared by Suelves *et al*. [188] using different concentrations of nano carbons produced from methane decomposition in a rotary. The study revealed the possibility of using nano carbons in polymer composites. Pinilla *et al*. [201] investigated using solar energy as a source of the heat for the decomposition reaction. Nano-carbon is formed using Ni/ Al_2O_3 and Fe/ Al_2O_3 and amorphous carbon is formed when using carbon as a catalyst.

Conclusions

In the nearest future, hydrogen production most probably will continue to rely on fossil fuels, chiefly, natural gas. Presently, hydrogen production technologies produce considerable amounts of CO_2 emissions. An environmentally smart technique for producing valuable carbon and pure hydrogen without (or with significantly reduced) CO_2 emissions is the thermo-catalytic decomposition of methane Carbon blacks, carbon fibers, carbon flakes and carbon nanotubes are the carbon products associated with hydrogen.

The valuable carbon byproducts could be sold, thus decreasing the net price of hydrogen production. The operating conditions and the type of catalyst used affect the value of the carbon formed in the catalytic methane decomposition. There is a strong relationship between the morphology of the formed carbon and its performance. Catalytic methane decomposition produces carbon nanotubes that possess surprising properties: high thermal and electrical conductivities, harder than diamond and many-times stronger than steel. It can be used as a structural material, catalyst, and catalyst support. It is also useful to the carbon fuel cell in forming the consuming anode.

The endothermicity reaction of methane decomposition is not very high. The thermodynamic data exhibit that the methane decomposition could be effected at moderate temperatures in the presence of appropriate catalysts. Comparison among transition metals shows that the catalytic performance order comes as: Ni > Co >Fe

At the beginning of the catalytic methane decomposition very high methane conversions could be obtained from the Fe-based catalyst by operating at a sufficiently high temperature. The formation of well-arranged graphitic carbon at 600°C benefits from Cu inclusion in the incipient alloyed Ni–Cu Raney-type catalysts .

Support structure and its textural features affect the conversion process so that unsupported catalysts are less active than the supported catalysts.

Carbon-based materials are considered as ideal catalysts for catalytic methane decomposition due to desirable features such as low material cost, high surface area, thermal stability, resistant to sulfur and other potentially detrimental impurities in the feedstock and can be easily separated from reaction system. A pore blockage and surface area reduction carbonaceous deposit of methane is commonly related to the loss of catalytic activity of carbon catalysts.

Acknowledgements

The authors thankfully acknowledge their appreciation to King Abdul-Aziz City for Science

and Technology (KACST) for funding the work through the research project # AT-34-4.

References

1. C. Böhringer and P. E. P. Joche, Measuring the Immeasurable a Survey of Sustainability Indices, *Ecolo. Econ*., **63**, 1(2007).
2. Y. Xing, R. Malcolm, W. Horner, M. A. El-Haram and J. Bebbington, A Framework Model for Assessing Sustainability Impacts of Urban Development, *Acc. Forum*, **33**, 209 (2009).
3. N. Lior, Sustainable Energy Development: The Present (2009) Situation and Possible Paths to the Future, *Energy*, **35**, 3976 (2010).
4. IEA, *Building the Cost Curves for the Industrial Sources of Non CO_2 Greenhouse Gases. Greenhouse Gas R&D Program*, Report No. PH_4/ 25, OECD, Paris, (2003).
5. M. J. Benton and A. J. Newell, Impacts of Global Warming on Permo-Triassic Terrestrial Ecosystems, *Gond. Res.*, **25**, 1308 (2014).
6. G. R. Lima, M. S. Sthel, J. R. Tavares, D. U. Schramm, M. G. da Silva and H. Vargas, Detection of Gaseous Pollutants by VNG-Powered Vehicles, *Procedia Environ. Sci.*, **4**, 61 (2011).
7. M. Höök, J. Li, K. Johansson and S. Snowden, Growth Rates of Global Energy Systems and Future Outlooks, *Nat. Resour. Res.*, **21**, 23 (2012).
8. M. Ana, López-Sabirón, A. Aranda-Usón, M. D. Mainar-Toledo, V. J. Ferreira and G. Ferreira, Environmental Profile of Latent Energy Storage Materials Applied to Industrial Systems, *Sci. Total Environ.*, **473**, 565 (2014).
9. L. Huimin, The impact of Human Behavior on Ecological Threshold: Positive or negative?—Grey Relational Analysis of Ecological Footprint, *Energy Policy*, **56**, 711 (2013).
10. T. H. Ortmeyer and P. Pillay, Trends in Transportation Sector Technology Energy Use and Greenhouse Gas Emissions, *Proceedings of IEEE*, **89**, 1837 (2001).
11. P. P. Edwards, V. L. Kuznetsov, W. I. F. David and N. P. Brandon, Hydrogen and Fuel Cells: Towards a Sustainable Energy Future Energy Policy, *Energy Policy*, **36**, 4356 (2008).
12. W. R. Moomaw, Industrial Emissions of Greenhouse Gases, *Energy Policy*, **24**, 951 (1996).
13. B. G. Pollet, I. Staffell, J. L. Shang and V. Molkov, Fuel-cell (hydrogen) Electric Hybrid Vehicles: Alternative Fuels and Advanced Vehicle Technologies for Improved Environmental performance, WoodHead Publishing Series, p.685 (2014).
14. T. M. I. Mahlia and P. L. Chan, Life Cycle Cost Analysis of Fuel Cell Based Cogeneration System for Residential Application in Malaysia, *Renew. Sust. Energ. Rev*., **15**, 416 (2011).
15. I. Mansouri and R. K. Calay, Materials Handling Vehicles; an Early Market Sector for Hydrogen Fuel Cells within Europe, *Sustainable Vehicle Technologies, Driving the Green Agenda*, Cambridge, UK: Woodhead Publishing Limited, p.99 (2012).
16. N. De Miguel, J. Manzanedo and P. L. Arias, Active and Stable Ni-MgO Catalyst Coated on a Metal Monolith for Methane Steam Reforming Under Low Steam-to-Carbon Ratios, *Chem. Eng. Technol*., **35**, 2195 (2012).
17. C. Mateos-Pedrero, S. R. González-Carrazán, M. A. Soria and P. Ruíz, Effect of the Nature of TiO_2 Support Over the Performances of Rh/TiO_2 Catalysts in the Partial Oxidation of Methane, *Catal. Today*, **203**, 158 (2013).
18. U. Izquierdo, V. L. Barrio, J. F. Cambra, J. Requies, M. B. Güemez, P. L. Arias, G. Kolb, R. Zapf, A. M. Gutiérrez and J. R. Arraib, Hydrogen Production from Methane and Natural Gas Steam Reforming in Conventional and Microreactor Reaction Systems, *Int. J. Hydrogen Energy*, **37**,7026 (2012).
19. D. K. Lee, K. Y. Koo, D. J. Seo and W. L. Yoon, Analysis of Design Variables for an Efficient Natural Gas Steam Reforming Process Comprised in a Small Scale Hydrogen Fueling Station, *Renew. Energy*, **42**, 234 (2012).
20. E. A. Sanchez and R. A. Comell, Hydrogen by Glycerol Steam Reforming on a Nickel–Alumina Catalyst: Deactivation Processes and Regeneration, *Int. J. Hydrogen Energy*, **37**, 14740 (2012).
21. O. Korup, C. F. Goldsmith, G. Weinberg, M. Geske, T. Kandemir, R. Schlögl and R. Horn, Catalytic Partial Oxidation of Methane on Platinum Investigated by Spatial Reactor Profiles, Spatially Resolved Spectroscopy, and Microkinetic Modeling, *J. Catal*., **297**, 1 (2013).
22. F. J. Wang, S. Zhang, Z. D. Chen, C. Liu and Y. G. Wan, Tar Reforming using Char as Catalyst During Pyrolysis and Gasification of Shengli Brown Coal, *J. Anal. Appl. Pyrol*., **105**, 269 (2014).
23. D. J. Roddy, A Syngas Network for Reducing Industrial Carbon Footprint and Energy Use, *Appl. Therm. Eng*., **53**, 299 (2013).
24. P. M. Sforza, A. Castrogiovanni, R. Voland, Coal-Derived Syngas Purification and Hydrogen Separation in a Supersonic Swirl Tube, *Appl. Therm. Eng*., **49**, 154 (2012).

25. J. Zhang, Ph.D. Dissertation, *Investigation of CO Tolerance in Proton Exchange Membrane Fuel Cells*, Worcester Polytechnic Institute, (2004).
26. H. Meng, N. Larouche, M. Lefèvre, F. Jaouen, B. Stansfield and J. P. Dodele, Iron Porphyrin-Based Cathode Catalysts for Polymer Electrolyte Membrane Fuel Cells: Effect of NH_3 and Ar Mixtures as Pyrolysis Gases on Catalytic Activity and Stability, *Electrochim. Acta*, **55**, 6450 (2010).
27. A. E. Awadallah, M. S. Mostafa, A. A. Aboul-Enein and S. A. Hanafi, Hydrogen Production via Methane Decomposition Over Al_2O_3–TiO_2 Binary Oxides Supported Ni Catalysts: Effect of Ti Content on the Catalytic Efficiency, *Fuel*, **129**, 68 (2014).
28. V. Shilapuram, N. Ozalp, M. Oschatz, L. Borchardt and S. Kaske, 'Hydrogen Production from Catalytic Decomposition of Methane over Ordered Mesoporous Carbons (CMK-3) and Carbide-Derived Carbon (DUT-19), *Carbon*, **67**, 377 (2014).
29. P. Ammendola, R. Chirone, G. Ruoppolo and G. Russ, Production of Hydrogen from Thermo-Catalytic Decomposition of Methane in a Fluidized Bed Reactor, *Chem. Eng. J*., **154**, 287 (2009).
30. J. L. Pinilla, R. Utrilla, M. J. Lázaro, R. Moliner, I. Suelves and A. B. García, Ni- and Fe-Based Catalysts for Hydrogen and Carbon Nanofilament Production by Catalytic Decomposition of Methane in a Rotary Bed Reactor, *Fuel Process. Technol*., **92**, 1480 (2011).
31. I. Alig, P. Pötschke, D. Lellinger, T. Skipa, S. Pegel, G. R. Kasaliwal and T. Villmo, Establishment, Morphology and Properties of Carbon Nanotube Networks in Polymer Melts, *Polymer*, **53**, 4 (2012).
32. J. Zhu, J. Jia and S. C. Tjong, *Preparation, Structure, and Application of Carbon Nanotubes/Bamboo Charcoal Composite,in "Nanocrystalline Materials"*, (2nd Edition) Chapter 1, Elsevier, p. 1 (2014).
33. M. Roy, *Nanocrystalline and Disordered Carbon Materials*, *Functional Materials*, Elsevier, p. 675 (2012).
34. H. Ichi-oka, N. Higashi, Y. Yamada, T. Miyake and T. Suzuki, Carbon Nanotube and Nanofiber Syntheses by the Decomposition of Methane on group 8–10 metal-loaded MgO catalysts, *Diam. Relat. Mater*., **16**, 1121 (2007).
35. R. Guil-Lo´pez, V. La Parola, M. A. Pen˜a and J. L. G. Fierro, Evolution of the Ni-Active Centres into Ex Hydrotalcite Oxide Catalysts During the COx-Free Hydrogen Production by Methane Decomposition, *Int. J. Hydrogen Energy*, **37**, 7042 (2012).
36. G. B. Nuremberg, H. V. Fajardo, D. Z. Mezalira, T. J. Casarin, L. F. D. Probst and N. V. Carren˜o, Preparation and Evaluation of Co/Al_2O_3 Catalysts in the Production of Hydrogen from Thermocatalytic Decomposition of Methane: Influence of Operating Conditions on Catalyst Performance, *Fuel*, **87**, 1698 (2008).
37. I. Suelves, M. J. La´zaro, R. Moliner, Y. Echegoyen and J. M. Palacios, Characterization of NiAl and NiCuAl Catalysts Prepared by Different Methods for Hydrogen Production by Thermo Catalytic Decomposition of Methane, *Catal. Today*, **116**, 271 (2006).
38. S. Takenaka, M. Serizawa and K. Otsuka, Formation of Filamentous Carbons over Supported Fe Catalysts Through Methane Decomposition, *J. Catal*., **222**, 520 (2004).
39. D. P. Serrano, J. Á. Botas, P. Pizarro and G. Góme, Kinetic and Autocatalytic Effects During the Hydrogen Production by Methane Decomposition over Carbonaceous Catalysts, *Int. J. Hydrogen Energy*, **38**, 5671 (2013).
40. J. M. Gatica, D. M. Gómez, S. Harti and H. Vida, Monolithic Honeycomb Design Applied to Carbon Materials for Catalytic Methane Decomposition, *Appl. Catal. A: Gen*., **458**, 21 (2013).
41. J. A. Botas, D. P. Serrano, R. Guil-López, P. Pizarro and G. Góme, Methane Catalytic Decomposition over Ordered Mesoporous Carbons: A Promising Route for Hydrogen Production, *Int. J. Hydrogen Energy*, **35**, 9788 (2010).
42. A. A. Al-Hassani, H. F. Abbas and W. M. A. W. Daud, Hydrogen Production Via Decomposition of Methane Over Activated Carbons as Catalysts: Full Factorial Design, *Int. J. Hydrogen Energy*, **39**, 7004 (2014).
43. S. P. Chai, S. H. S. Zein and A. R. Mohamed, *A Review on Carbon Nanotubes Production via Catalytic Methane Decomposition*,1st National Postgraduate Colloquim (NAPCOL), School of Chemical Engineering,, USM Malysia, p.60 (2004).
44. M. Kumar and Y. Ando, Chemical Vapor Deposition of Carbon Nanotubes: A Review on Growth Mechanism and Mass Production, *J. Nanosc. Nanotechnol*. **10**, 3739 (2010).
45. Y. Li, D. Li and G. Wang, Methane decomposition to COx-free hydrogen and nano-carbon material on group 8–10 base metal catalysts: A review, *Catal. Today*, **162**, 1 (2011).
46. H. F. Abbas and W. M. A. W. Daud, Hydrogen Production by Methane Decomposition: A

review, *Int. J. Hydrogen Energy*, **35**, 1160 (2010).
47. A. M. Amin, E. Croiset and W. Epling, Review of Methane Catalytic Cracking for Hydrogen Production, *Int. J. Hydrogen Energy*, **36**, 2904 (2011).
48. S. Ahmed, A. Aitani, F. Rahman, A. Al-Dawood and F. Al-Muhaish, Decomposition of Hydrocarbons to Hydrogen and Carbon, *Appl. Catal. A*: *Gen*., **359**, 1 (2009).
49. A. Abánades, C. Rubbia and D. Salmieri, Technological Challenges for Industrial Development of Hydrogen Production Based on Methane Cracking, *Energy*, **46**, 359 (2012).
50. A. Abanades, C. Rubbia and D. Salmieri, Thermal Cracking of Methane into Hydrogen for a CO_2-Free Utilization of Natural Gas, *Int. J. Hydrogen Energy*, **38**, 8491 (2013).
51. R. Guil-Lopez, J. A. Botas, J. L. G. Fierro and D. P. Serrano, Comparison of Metal and Carbon Catalysts for Hydrogen Production by Methane Decomposition, *Appl. Catal.* A*: Gen.*, **396**, 40 (2011).
52. M. Serban, M. A. Lewis, C. L. Marshall and R. D. Doctor, Hydrogen Production by Direct Contact Pyrolysis of Natural Gas, *Energy Fuel*, **17**, 705 (2003).
53. M. H. Kim, E. K. Lee, J. H. Jun, S. J. Kong, G. Y. Han and B. K. Lee, Hydrogen Production by Catalytic Decomposition of Methane Over Activated Carbons: Kinetic Study, *Int. J. Hydrogen Energy*, **29**, 187 (2004).
54. N. Z. Muradov, How to Produce Hydrogen from Fossil Fuels without CO_2 Emission, *Int. J. Hydrogen Energy*, **18**, 211 (1993).
55. Y. Zhorov, *Thermodynamics of Chemical Processes*. Khimiya, Moscow, **91**, 263 (1985).
56. M. Andier and M. Coulon, Kinetic and Microscopic Aspects of Catalytic Carbon Growth, *Carbon*, **23**, 317 (1985).
57. J. R. Rostrup-Nielsen, Equilibria of Decomposition Reactions of Carbon Monoxide and Methane Over Nickel Catalysts, *J. Catal*., **27**, 343 (1972).
58. I. Alstrup, A New Model Explaining Carbon Filament Growth on Nickel, Iron, and NieCu Alloy Catalysts, *J. Catal*., **109**, 241 (1988).
59. S. Fukada, N. Nakamura, J. Monden and M. Nishikawa, Experimental Study of Cracking Methane by Ni/SiO_2 Catalyst, *J. Nucl. Mater.*, **329-333**, 1365 (2004).
60. A. V. Krestinin, A. V. Raevskii and M. B. Kislov, A New Model Explaining Carbon Filament Growth on Nickel, Iron, and Ni-Cu Alloy Catalysts, *Carbon*, **46**, 1450 2008).
61. R. T. K. Baker, M. A. Barber, P. S. Harris, F. S. Feates and R. J. Waite, Nucleation and Growth of Carbon Deposits from the Nickel Catalyzed Decomposition of Acetylene, *J. Catal*., **26**, 51 (1972).
62. A. J. Sacco, P. Thacker, T. N. Chang and A. T. S. Chiang, The Initiation and Growth of Filamentous Carbon from α-Iron in H_2, CH_4, CO_2 and CO Mixtures, *J. Catal*., **85**, 224 (1984).
63. R. T. Yang and J. P. Chen, Mechanism of Carbon Filament Growth on Metal Catalysts, *J. Catal*., **115**, 52 (1989).
64. R. T. Yang, P. J. Goethel, J. M. Schwartz and C. R. F. Lund, Solubility and Diffusivity of Carbon in Metals, *J. Catal*., **122**, 206 (1990).
65. J. I. Villacampa, C. Royo, E. Romeo, J. A. Montoya, P. Del Angel and A. Monzo´n, A. Catalytic Decomposition of Methane Over Ni-Al_2O_3 Coprecipitated Catalysts: Reaction and Regeneration Studies, *Appl. Catal. A:Gen.*, **252**, 363 (2003).
66. Y. Zhang and K. J. Smith, Carbon Formation Thresholds and Catalyst Deactivation during CH_4 Decomposition on Supported Co and Ni catalysts, *Catal Lett*., **95**, 7 (2004).
67. J. W. Snoeck, G. F. Froment and M. Fowles, Filamentous Carbon Formation and Gasification: Thermodynamics, Driving Force, Nucleation, and Steady-State Growth, *J. Catal*., **169**, 240 (1997).
68. M. A. Ermakova, D. Y. Ermakov and G. G. Kuvshinov, Effective Catalysts for Direct Cracking of Methane to Produce Hydrogen and Filamentous Carbon: Part I. Nickel catalysts, *Appl. Catal. A:Gen.*, **201**, 61 (2000).
69. T. Zhang and M. D. Amiridis, Hydrogen Production via the Direct Cracking of Methane Over Silica-Supported Nickel Catalysts, *Appl. Catal. A:Gen.*, **167**, 161 (1998).
70. M. A. Ermakova and D. Y. Ermakov, Ni/SiO_2 and Fe/SiO_2 Catalysts for Production of Hydrogen and Filamentous Carbon via Methane Decomposition, *Catal. Today*, **77**, 225 (2002).
71. L. B. Avdeeva, T. V. Reshetenko, Z. R. Ismagilov and V. A. Likholobov, Iron-Containing Catalysts of Methane Decomposition: Accumulation of Filamentous Carbon, *Appl. Catal. A:Gen.*, **228**, 53 (2002).
72. M. Pudukudy and Z. Yaakob, Methane Decomposition Over Ni, Co and Fe Based Monometallic Catalysts Supported on Sol Gel Derived SiO_2 Microflakes, *Chem. Eng. J.*, **262**, 1009 (2015).
73. M. Pudukudy, Z. Yaakob and Z. S. Akmal, Direct Decomposition of Methane over SBA-15 Supported Ni, Co and Fe based Bimetallic Catalysts, *Appl. Surf. Sci.*, **330**, 418 (2015).
74. M. N. Uddin, W. M. A. W. Daud and H. F. Abbas, Co-Production of Hydrogen and Carbon

Nanofibers from Methane Decomposition over Zeolite Y Supported Ni Catalysts, *Energy Conv. Manag.*, **90**, 218 (2015).
75. Y. Shen and A. C. Lua, Sol–Gel Synthesis of Titanium Oxide Supported Nickel Catalysts for Hydrogen and Carbon Production by Methane Decomposition, *J. Power Sources*, **280**, 467 (2015).
76. Y. Shen and A. C. Lua, Polyol Synthesis of Nickel–Copper Based Catalysts for Hydrogen Production by Methane Decomposition, *Int. J. Hydrogen Energy*, **40**, 311 (2015).
77. H. Y. Wang and A. C. Lua, Methane Decomposition using Ni–Cu Alloy Nano-Particle Catalysts and Catalyst Deactivation Studies, *Chem. Eng. J.*, **262**, 1077 (2015).
78. A. H. Fakeeha, W. U. Khan, A. S. Al-Fatesh, A. E. Abasaeed and M. A. Naeem, Production of Hydrogen and Carbon Nanofibers from Methane over Ni–Co–Al catalysts, *Int. J. Hydrogen Energy*, **40**, 1774 (2015).
79. Y. Ying, C. Meisheng, L. Minglai, Z. Na, L. Zhiqi and S. Yongxi, Rare Earth Modified Ni-Si Catalysts for Hydrogen Production from Methane Decomposition, *J. Rare Earth.*, **32**, 709 (2014).
80. A. E. Awadallah, A. A. Aboul-Enein and A. K. Aboul-Gheit, Impact of Group VI Metals Addition to Co/MgO Catalyst for Non-Oxidative Decomposition of Methane into COx-free Hydrogen and Carbon Nanotubes, *Fuel*, **129**, 27 (2014).
81. Y. Li, B. Zhang, X. Xie, J. Liu, Y. Xu and W. Shen, Novel Ni Catalysts for Methane Decomposition to Hydrogen and Carbon Nanofibers, *J. Catal*., **238**, 412 (2006).
82. M. Cai, Y. Li, W. Shen, J. Rogers, WO Patent No. 2007/100333, September 7, (2007).
83. P. Colombani, E. Cremonesi, EP Patent 1227062, July 31, (2002).
84. M. S. Rahman, E. Croiset and R. R. Hudgins, Catalytic Decomposition of Methane for Hydrogen Production, *Top. Catal.*, **37**, 137 (2006).
85. A. C. Lua and H. Y. Wang, Hydrogen Production by Catalytic Decomposition of Methane over Ni-Cu-Co Alloy Particles, *Appl. Catal. B:Environ.*, **156**, 84 (2014).
86. W. Wang, H. Wang, Y. Yang and S. Jiang, Ni–SiO_2 and Ni–Fe–SiO_2 Catalysts for Methane Decomposition to Prepare Hydrogen and Carbon Filaments, *Int. J. Hydrogen Energy*, **37**, 9058 (2012).
87. A. Venugopal, K. S. Naveen, J. Ashok, P. D. Hari, K. V. Durga and K. B. S. Prasad, Hydrogen Production by Catalytic Decomposition of Methane over Ni/SiO_2, *Int. J. Hydrogen Energy*, **32**, 1782 (2007).
88. I. Suelves, M. J. La´zaro, R. Moliner, B. M. Corbella and J. M. Palacios, Hydrogen Production by Thermo Catalytic Decomposition of Methane on Ni-Based Catalysts: Influence of Operating Conditions on Catalyst Deactivation and Carbon Characteristics, *Int. J. Hydrogen Energy*, **30**, 1555 (2005).
89. H. Ogihara, S. Takenaka, I. Yamanaka, E. Tanabe, A. Genseki and K. Otsuka, Formation of Highly Concentrated Hydrogen Through Methane Decomposition over Pd-Based Alloy Catalysts, *J. Catal*., **238**, 353 (2006).
90. G. B. Nuernberg, H. V. Fajardo, D. Z. Mezalira, T. J. Casarin, L. F. D. Probst and N. L. V. Carreño, Preparation and Evaluation of Co/Al_2O_3 Catalysts in the Production of Hydrogen from Thermo-Catalytic Decomposition of Methane: Influence of Operating Conditions on Catalyst Performance, *Fuel*, **87**, 1698 (2008).
91. P. Jana, V. A. de la Peña O'Shea, J. M. Coronado and D. P. Serrano, Mild Temperature Hydrogen Production by Methane Decomposition over Cobalt Catalysts Prepared with Different Precipitating Agents, *Int. J. Hydrogen Energy*, **37**, 7034 (2012).
92. H. Y. Wang and E. Ruckenstein, *Carbon*, Formation of Filamentous Carbon During Methane Decomposition over Co–MgO Catalysts **40**, 1911 (2002).
93. P. Jana, V. A. de la P. O'Shea, J. M. Coronado and D. P. Serrano, H_2 Production by CH_4 Decomposition over Metallic Cobalt Nanoparticles: Effect of the Catalyst Activation, *Appl. Catal. A:Gen.*, **467**, 371 (2013).
94. L. Piao, J. Chen and Y. Li, Carbon Nanotubes via Methane Decomposition on an Alumina Supported Cobalt Aerogel Catalyst, *China Part.*, **1**, 266 (2003).
95. L. B. Avdeeva, D. I. Kochubey and S. K. Shaikhutdinov, Cobalt Catalysts of Methane Decomposition: Accumulation of the Filamentous Carbon, *Appl. Catal. A:Gen.*, **177**, 43 (1999).
96. Y. Zhang and K. J. Smith, CH_4 Decomposition on Co Catalysts: Effect of Temperature, Dispersion, and the Presence of H_2 or CO in the feed, *Catal. Today*, **77**, 257 (2002).
97. I. Abdullahi, N. Sakulchaicharoen and J. E. Herrera, Selective Synthesis of Single-Walled Carbon Nanotubes on Fe–MgO Catalyst by Chemical Vapor Deposition of Methane, *Diam. Relat. Mater.*, **41**, 84 (2014).

98. J. L. Pinilla, R. Utrilla, R. K. Karn, I. Suelves, M. J. Lázaro, R. Moliner, A. B. García and J. N. Rouzaud, High Temperature Iron-Based Catalysts for Hydrogen and Nanostructured Carbon Production by Methane Decomposition, *Int. J. Hydrogen Energy*, **36**, 7832 (2011).
99. L. Tang, D. Yamaguchi, N. Burke, D. Trimma and K. Chiang, Methane Decomposition Over Ceria Modified Iron Catalysts, *Catal. Commun.*, **11**, 1215 (2010).
100. W. Gac, A. Denis, T. Borowiecki and L. Kepinski, Methane Decomposition Over Ni-MgO-Al_2O_3 Catalysts, *Appl. Catal. A:Gen.*, **357**, 236 (2009).
101. Y. D. Li, J. L. Chen and L. Chang, Catalytic Growth of Carbon Fibers from Methane on a Nickel–Alumina Composite Catalyst Prepared from Feitknecht Compound Precursor, *Appl. Catal. A: Gen*., **163**, 45 (1997).
102. M. L. Toebes, J. H. Bitter, A. J. van Dillen and K. P. de Jong, Impact of the Structure and Reactivity of Nickel Particles on the Catalytic Growth of Carbon Nanofibers, *Catal. Today*, **76**, 33 (2002).
103. Y. Echegoyen, I. Suelves, M. J. La´zaro, R. Moliner and J. M. Palacios, Hydrogen Production by Thermocatalytic Decomposition of Methane over Ni-Al and Ni-Cu-Al Catalysts: Effect of Calcination Temperature, *J. Power Sources*, **169**, 150 (2007).
104. S. Takenaka, H. Ogihara, I. Yamanaka and K. Otsuka, Decomposition of Methane Over Supported-Ni Catalysts: Effects of the Supports on the Catalytic Lifetime, *Appl. Catal. A:Gen.*, **217**, 101 (2001).
105. Y. Li, B. Zhang, X. Tang, Y. Xu and W. Shen, Hydrogen Production from Methane Decomposition over Ni/CeO_2 catalysts, *Catal. Commun*., **7**, 380 (2006).
106. S. Takenaka, M. Ishida, M. Serizawa, E. Tanabe and K. Otsuka, Formation of Carbon Nanofibers and Carbon Nanotubes through Methane Decomposition over Supported Cobalt Catalysts, *J. Phys. Chem. B*, **108**, 11464 (2004).
107. G. Bonura, O. D. Blasi, L. Spadaro, F. Arena and F. Frusteri, A Basic Assessment of the Reactivity of Ni Catalysts in the Decomposition of Methane for the Production of "COx-free" Hydrogen for Fuel Cells Application, *Catal. Today*, **116**, 298 (2006).
108. Y. H. Hu and E. Ruckenstein, Binary MgO-Based Solid Solution Catalysts for Methane Conversion to syngas, *Catal. Rev. Sci. Eng*., **44**, 423 (2002).
109. Z. R. Ismagilov, N. V. Shikina, V. N. Kruchinin, N. A. Rudina, V. A. Ushakov, N. T. Vasenin and H. J. Veringa, Development of Methods of Growing Carbon Nanofibers on Silica Glass Fiber Supports, *Catal. Today*, **102**, 85 (2005).
110. L. Chen, H. T. Liu, K. Yang, J. K. Wang and X. L. Wang, Catalytic Synthesis of Carbon Nanotubes from the Decomposition of Methane over a Ni–Co/La_2O_3 catalyst, *Can. J. Chem*., **87**, 47 (2009).
111. M. Kuras, Y. Zimmermann and C. Petit, Reactivity of perovskite-type precursor in MWCNTs Synthesis, *Catal. Today*, **138**, 55 (2008).
112. G. S. Gallego, J. Barrault, C. Batiot-Dupeyrat and F. Mondragon, Production of Hydrogen and MWCNTs by Methane Decomposition over Catalysts Originated from $LaNiO_3$ perovskite, *Catal. Today*, **149**, 365 (2010).
113. M. E. Rivas, J. L G. Fierro, R. Guil-Lopez, M. A. Pena, V. La Parola and M. R. Goldwasser, Preparation and Characterization of Nickel-Based Mixed-Oxides and their Performance for Catalytic Methane Decomposition, *Catal. Today*, **133**, 367 (2008).
114. B. C. Liu, S. H. Tang, Z. L. Yu, B. L. Zhang, T. Chen and S. Y. Zhang, Catalytic Growth of Single-Walled Carbon Nanotubes with a Narrow Distribution of Diameters Over Fe Nanoparticles Prepared in situ by the Reduction of $LaFeO_3$, *Chem. Phys. Lett*., **357**, 297 (2002).
115. A. F. Cunha, N. Mahata, J. J. M. Orfao and J. L. Figueiredo, Methane Decomposition on La_2O_3-Promoted Raney-Type Fe Catalysts, *Energy Fuels*, **23**, 4047 (009).
116. J. L. Figueiredo, J J. M. Orfao and A. F. Cunha, Hydrogen Production via Methane Decomposition on Raney-Type Catalysts, *Int. J. Hydrogen Energy*, **35**, 9795 (2010).
117. E. Ruckenstein and Y. H. Hu, Catalytic Preparation of Narrow Pore Size Distribution Mesoporous Carbon, *Carbon*, **36**, 269 (1998).
118. T. V. Reshetenko, L. B. Avdeeva, Z. R. Ismagilov, A. L. Chuvilin, Catalytic Filamentous Carbon as Supports for Nickel Catalysts, *Carbon*, **42**, 143 (2004).
119. T. V. Reshetenko, L. B. Avdeeva, Z. R. Ismagilov, A. L. Chuvilin and V. B. Fenelonov, Catalytic Filamentous Carbons-Supported Ni for Low-Temperature Methane Decomposition, *Catal. Today*, **102**, 115 (1997).
120. S. K. Shaikhutdinov, L. B. Avdeeva, B. N. Novgorodov, V. I. Zaikovskii and D. I. Kochubey, Nickel Catalysts Supported on Carbon Nanofibers: Structure and Activity in Methane Decomposition, *Catal. Lett*., **47**, 35 (1997).

121. J. Ashok, S. N. Kumar, A. Venugopal, V. D. Kumari and M. Subrahmanyam, COx-free H_2 Production via Catalytic Decomposition of CH_4 over Ni Supported on Zeolite Catalysts, *J. Power Sources*, **164**, 809 (2007).
122. J. C. Guevara, J. A. Wang, L. F. Chen, M. A. Valenzuela, P. Salas, A. García-Ruiz, J. A. Toledo, M. A. Cortes-Jácome, C. Angeles-Chavez and O. Novaro, Ni/Ce-MCM-41 Mesostructured Catalysts for Simultaneous Production of Hydrogen and Nanocarbon Via Methane Decomposition, *Int. J. Hydrogen Energy*, **35**, 3509 (2010).
123. J. Ziebro, I. Lukasiewicz, E. Borowiak-Palen and B. Michalkiewicz, Low Temperature Growth of Carbon Nanotubes from Methane Catalytic Decomposition over Nickel Supported on a Zeolite, *Nanotechnology*, **21**, 145308 (2010).
124. J. M. Jehng, W. C. Tung and C. H. Kuo, The Formation Mechanisms of Multi-Wall Carbon Nanotubes over the Ni Modified MCM-41 Catalysts, *J. Porous Mater*., **15**, 43 (2008).
125. T. V. Choudhary, C. Sivadinarayana, C. C. Chusuei, A. Klinghoffer and D. W. Goodman, Hydrogen Production via Catalytic Decomposition of Methane, *J. Catal.*, **199**, 9 (2001).
126. T. V. Choudhary, C. Sivadinarayana, A. Klinghoffer and D. W. Goodman, Catalytic Decomposition of Methane: Towards Production of CO-Free Hydrogen for Fuel Cells, *Stud. Surf. Sci. Catal*., **136**, 197 (2001).
127. E. Odier, Y. Schuurman and C. Mirodatos, Non-Stationary Catalytic Cracking of Methane Over Ceria-Based Catalysts: Mechanistic Approach and Catalyst Optimization, *Catal. Today*, **127**, 230 (2007).
128. A. M. Cassell, J. A. Raymakers, J. Kong and H. J. Dai, Large Scale CVD Synthesis of Single-Walled Carbon Nanotubes, *J. Phys. Chem. B*, 103, 6484 (1999).
129. H. Ago, N. Uehara, N. Yoshihara, M. Tsuji, M. Yumura, N. Tomonaga and T. Setoguchi, Gas Analysis of the CVD Process for High Yield Growth of Carbon Nanotubes Over Metal-Supported Catalysts, *Carbon*, **44**, 2912 (2006).
130. S. Tang, Z. Zhong, Z. Xiong, L. Sun, L. Liu, J. Lin, Z. X. Shen and K. L. Tan, Controlled Growth of Single-Walled Carbon Nanotubes by Catalytic Decomposition of CH_4 over Mo/Co/MgO Catalysts, *Chem. Phys. Lett.*, **350**, 19 (2001).
131. L. Ni, K. J. Kuroda, L. P. Zhou, T. Kizuka, K. Ohta, K. Matsuishi and J. J. Nakamura, Kinetic Study of Carbon Nanotube Synthesis over Mo/Co/MgO Catalysts, *Carbon*, **44**, 2265 (2006).
132. Q. W. Li, H. Yan, Y. Cheng Yan, J. Zhang and Z. F. Liu, A Scalable CVD Synthesis of High-Purity Single-Walled Carbon Nanotubes with Porous MgO as Support Material, *J. Mater. Chem*., **12**, 1179 (2002).
133. G. Q. Ning, F. Wei, Q. Wen, G. H. Luo, Y. Wang and Y. Jin, Improvement of Fe/MgO Catalysts by Calcination for the Growth of Single- and Double-Walled Carbon Nanotubes, *J. Phys. Chem.* B, **110**, 1201 (2006).
134. G. Q. Ning, Y. Liu, F. Wei, Q. Wen and G. H. Luo, Porous and Lamella-like Fe/MgO catalysts prepared under hydrothermal conditions for high-yield synthesis of double-walled carbon nanotubes, *J. Phys. Chem. C*, **111**, 1969 (2009).
135. J. Q. Nie, W. Z. Qian, Q. Zhang, Q. Wen and F. Wei, Very high-quality single-walled carbon nanotubes grown using a structured and tunable porous Fe/MgO catalyst, *J. Phys. Chem. C*, **113**, 20178 2009).
136. M. Paillet, V. Jourdain, P. Poncharal, J. L. Sauvajol and A. Zahab, Versatile synthesis of individual single-walled carbon nanotubes from nickel nanoparticles for the study of their physical properties, *J. Phys. Chem. B*, **108**, 17112 (2004).
137. X. Wang, W. B. Yue, M. S. He, M. H. Liu, J. Zhang and Z. F. Liu, Bimetallic catalysts for the efficient growth of SWNTs on surfaces, *Chem. Mater*., **16**, 799 (2004).
138. Y. Li, J. Liu, Y. Q. Wang and Z. L. Wang, Preparation of monodispersed Fe–Mo nanoparticles as the catalyst for CVD synthesis of Carbon Nanotubes, *Chem. Mater*., **13**, 1008 (2001).
139. J. Kong, H. T. Soh, A. M. Cassell, C. F. Quate and H. J. Dai, Synthesis of individual single-walled carbon nanotubes on patterned silicon wafers, *Nature*, **395**, 878 (1998).
140. R. W. Coughlin, Carbon as adsorbent and catalyst, *Product R&D*, **8**, 12 (1969).
141. A. Domı´nguez, B. Fidalgo, Y. Ferna´ndez, J. J. Pis and J. A. Mene´ndez, Microwave-assisted catalytic decomposition of methane over activated carbon for CO2-free hydrogen production, *Int. J. Hydrogen Energy*, **32**, 4792 (2007).
142. R. Moliner, I. Suelves, M. J. Lázaro and O. Moreno, Thermocatalytic decomposition of methane over activated carbons: influence of textural properties and surface chemistry, *Int. J. Hydrogen Energy*, **30**, 293 (2005).
143. M. J. La´zaro, J. L. Pinilla, I. Suelves and R. Moliner, Study of the deactivation mechanism of

carbon blacks used in methane decomposition, *Int. J. Hydrogen Energy*, **33**, 4104 (2008).

144. H. F. Abbas and W. M. A. W. Daud, Thermocatalytic decomposition of methane for hydrogen production using activated carbon catalyst: regeneration and characterization studies, *Int. J. Hydrogen Energy*, **34**, 8034 (2009).
145. J. Planeix, N. Coustel, B. Coq, V. Brotons, P. Kumbhar, R. Dutartre, P. Geneste, P. Bernier and P. Aayan, Application of carbon nanotubes as supports in heterogeneous catalysis, *J. Am. Chem. Soc*., **116**, 7935 (1994).
146. P. Serp and E. Castillejos, Catalysis in carbon nanotubes, *ChemcatChem*, **2**, 41 (2010).
147. D. S. Su, J. Zhang, B. Frank, A. Thomas, X. Wang, J. Paraknowitsch and R. Schlogl, Metal-free heterogeneous catalysis for sustainable chemistry, *ChemSusChem*, **3**, 169 (2010).
148. N. Muradov, F. Smith and A.T-Raissi, Catalytic activity of carbons for methane decomposition reaction, *Catal. Today*, **102-103**, 225 (2005).
149. J. Zhang, L. Jin, Y. Li, H. Si, B. Qiu and H. Hu, Hierarchical porous carbon catalyst for simultaneous preparation of hydrogen and fibrous carbon by catalytic methane decomposition, *Int. J. Hydrogen Energy*, **38**, 8732 (2013).
150. A. Dufour, A. Celzard, V. Fierro, E. Martin, F. Broust and A. Zoulalian, Catalytic decomposition of methane over a wood char concurrently activated by a pyrolysis gas, *Appl. Catal. A*: *Gen*., **346**, 164 (2008).
151. P. Serp and J. L. Figueiredo, *Carbon Materials for Catalysis*, John Wiley & Sons, Hobo- ken, NJ, p. 131 (2009).
152. S. Abanades, H. Kimura and H. Otsuka, Hydrogen production from thermo-catalytic decomposition of methane using carbon black catalysts in an indirectly-irradiated tubular packed-bed solar reactor, *Int. J. Hydrogen Energy*, **39**, 18770 (2014).
153. P. Rechnia, A. Malaika, B. Krzyżyńska and M. Kozłowski, Decomposition of methane in the presence of ethanol over activated carbon catalyst, *Int. J. Hydrogen Energy*, **37**, 14178 (2012).
154. D. P. Serrano, J. A. Botas, J. L. G. Fierro, R. Guil-López, P. Pizarro and G. Gómez, Hydrogen production by methane decomposition: Origin of the catalytic activity of carbon materials, *Fuel*, **89**, 1241 (2010).
155. S. C. Lee, H. J. Seo and G. Y. Han, Hydrogen production by catalytic decomposition of methane over carbon black catalyst at high temperatures, *Korean J. Chem. Eng*., **30**, 1716 (2013).
156. S. Krzyzynski and M. Koz1owski, Activated carbons as catalysts for hydrogen production via methane decomposition, *Int. J. Hydrogen Energy*, **33**, 6172 (2008).
157. R. Guil-Lopez, J. A. Botas, J. L. G. Fierro and D. P. Serrano, Comparison of metal and carbon catalysts for hydrogen production by methane decomposition, *Appl. Catal. A: Gen.*, **396** 40 (2011).
158. D. Trimm., *Catal. Royal Soc. Chem*., **4**, 210 (1981).
159. N. Muradov, F. Smith, in: M. Marini and G. Spazzafumo, (Editors), *Hydrogen Power Theoretical nd Engineering Solutions*. SGEditoriali, Padova (Italy), p. 87 (2003).
160. J. Zhang, L. Jin, Y. Li and H. Hu, Ni doped carbons for hydrogen production by catalytic methane decomposition, *Int. J. Hydrogen Energy*, **38**, 3937 (2013).
161. J. Majewska and B. Michalkiewicz, Low temperature one-step synthesis of cobalt nanowires encapsulated in carbon, *Appl. Phys. A*, **111**, 1013 (2013).
162. P. Ammendolaa, R. Chirone, G. Ruoppolo and G. Russo, Production of hydrogen from thermo-catalytic decomposition of methane in a fluidized bed reactor, *Chem. Eng. J*., **154**, 287 2009).
163. N. Muradov, CO_2-free production of hydrogen by catalytic pyrolysis of hydrocarbon fuel, *Energy Fuel*, **12**, 41 (1998).
164. A. Monzón, N. Latorre, T. Ubieto, C. Royo, E. Romeo, J. I. Villacampa, L. Dussault, J. C. Dupin, C. Guimon and M. Montioux, Improvement of activity and stability of Ni–Mg–Al catalysts by Cu addition during hydrogen production by catalytic decomposition of methane, *Catal. Today*, **116**, 264 (2006).
165. O. Levenspiel, *Chemical reaction engineering*. (3rd ed.) Wiley, New York,; p. 475 (1999).
166. J. L. Pinilla, I. Suelves, M. L. La´zaro and R. Moliner, Kinetic study of the thermal decomposition of methane using carbonaceous catalysts, *Chem. Eng. J.*, **138**, 301 (2007).
167. M. J. La´zaro, J. L. Pinilla, I. Suelves and R. Moliner, Study of the deactivation mechanism of carbon blacks used in methane decomposition, *Int. J. Hydrogen Energy*, **33**, 4104 (2008).
168. J. S. Prasad, V. Dhand, V. Himabindu, Y. Anjaneyulu, P. K. Jain and B. Padya, Production of hydrogen and carbon nanofibers through the decomposition of methane over activated carbon supported Pd catalysts, *Int. J. Hydrogen Energy*, **35**, 10977 (2010).

169. V. Sariboga and F. Öksüzömer, The investigation of active Ni/YSZ interlayer for Cu-based direct-methane solid oxide fuel cells, *Appl. Energy*, **93**, 707 (2012).
170. J. L. Chen, M. He, G. W. Wang, Y. D. Li and Z. H. J. Zhu, Production of hydrogen from methane decomposition using nanosized carbon black as catalyst in a fluidized-bed reactor, *Int. J. Hydrogen Energy*, **34**, 9730 (2009).
171. U. Narkiewicz, M. Podsiadly, R. Jedrzejewski and I. Pelech, Catalytic decomposition of hydrocarbons on cobalt, nickel and iron catalysts to obtain carbon nanomaterials, *Appl. Catal. A: Gen*., **384**, 27 (2010).
172. R. Benito, M. Herrero, F. M. Labajos, V. Rives, C. Royo and N. Latorre, Production of carbon nanotubes from methane Use of Co–Zn–Al catalysts prepared by microwave-assisted synthesis, *Chem. Eng. J.*, **149**, 455 (2009).
173. M. Inoue, K. Asai, Y. Nagayasu, K. Takane, S. Iwamoto and E. Yagasaki, Formation of multi-walled carbon nanotubes by Ni-catalyzed decomposition of methane at 600–750 °C, *Diam. Relat. Mater.*, **17**, 1471 (2008).
174. N. de Jonge and J. M. Bonard, Carbon nanotube electron sources and applications, *Philos. T. Roy. Soc. A*, **362**, 2239 (2004).
175. X. Li, G. Zhu, S. Qi, J. Huang and B. Yang, Simultaneous production of hythane and carbon nanotubes via catalytic decomposition of methane with catalysts dispersed on porous supports, *Appl. Energy*, **130**, 846 (2014).
176. S. K. Saraswat and K. K. Pant, Synthesis of carbon nanotubes by thermo catalytic decomposition of methane over Cu and Zn promoted Ni/MCM-22 catalyst, *J. Environ. Chem. Eng.*, **1**, 746 (2013).
177. A. F. Cunha, J. J. M. Órfão and J. L. Figueiredo, Methane decomposition on Fe–Cu Raney-type catalysts, *Fuel Process. Technol.*, 90, 1234 (2009).
178. Z. Zhang, T. Tang, G. Lu, C. Qin, H. Huang and S. Zheng, Production of Hydrogen and Carbon Nanofiber via Methane Decomposition, *World Academy of Science, Engineering and Technology*, **4**, 05 (2010).
179. J. L. Figueiredo, J. J. M. O´rfa˜o and A. F. Cunha, Hydrogen production via methane decomposition on Raney-type catalysts, *Int. J. Hydrogen Energy* **35**, 9795 (2010).
180. V. V. Chesnokov and A. S. Chichkan, Production of hydrogen by methane catalytic decomposition over Ni–Cu–Fe/Al_2O_3 catalyst, *Int. J. Hydrogen Energy*, **34**, 2979 (2009).
181. J. L. Pinilla, R. Moliner, I. Suelves, M. J. Lazaro, Y. Echegoyen and J. M. Palacios, Production of hydrogen and carbon nanofibers by thermal decomposition of methane using metal catalysts in a fluidized bed reactor, *Int. J. Hydrogen Energy*, **32**, 4821 (2007).
182. D. Torres, J. L. Pinilla, M.J. Lázaro, R. Moliner and I. Suelves, Hydrogen and multiwall carbon nanotubes production by catalytic decomposition of methane: Thermogravimetric analysis and scaling-up of Fe–Mo catalysts, *Int. J. Hydrogen Energy*, **39**, 3698 (2014).
183. R. Aiello, J. E. Fiscus, H-C.Z. Loye and M. D. Amiridis, Hydrogen production via the direct cracking of methane over Ni/SiO_2: catalyst deactivation and regeneration, *Appl. Catal. A*: *Gen.*, **192**, 227 (2000).
184. J. Xiong, X. Dong, Y. Dong and X. Hao, Stuart Hampshire Dual-production of nickel foam supported carbon nanotubes and hydrogen by methane catalytic decomposition, *Int. J. Hydrogen Energy*, **37**, 12307 (2012).
185. A. E. Awadallah, S. M. Abdel-Hamid, D. S. El-Desouki, A. A. Aboul-Enein and A. K. Aboul-Gheit, Synthesis of carbon nanotubes by CCVD of natural gas using hydrotreating catalysts, *Egypt. J. Petrol.*, **21**, 101 (2012).
186. A.B. Garciaa, I. Camea, I. Suelves, J. L. Pinill, M. J. La´ zaro, J. M. Palacios and R. Moliner, The graphitization of carbon nanofibers produced by the catalytic decomposition of natural gas, *Carbon*, **47**, 2563 (2009).
187. S- P. Chai, S. H. S. Zein and A. R. Mohamed, COx-Free Hydrogen and Carbon Nanofibers Produced from Direct Decomposition of Methane on Nickel-Based Catalysts, *J. Nat. Gas Chem.*, **15**, 253 (2006).
188. I. Suelves, R. Utrilla, D. Torres, S. de Llobet, J. L. Pinilla, M. J. Lázaro and R. Moliner, Preparation of polymer composites using nanostructured carbon produced at large scale by catalytic decomposition of methane, *Mater. Chem. Phy.*, **137**, 859 (2013).
189. D. P. Serrano, J. A. Botas, P. Pizarro, R. Guil-Lopez and G. Gomez, Ordered mesoporous carbons as highly active catalysts for hydrogen production by CH_4 decomposition, *Chem. Commun*., **48**, 6585 (2008).
190. B. H. Ryu, S. Y. Lee, D. H. Lee, G. Y. Han, T. J. Lee and K. J. Yoon, Catalytic characteristics of various rubber-reinforcing carbon blacks in decomposition of methane for hydrogen production, *Catal. Today*, **123,** 303 (2007).
191. I. Suelves, J. L. Pinilla, M. J. Lázaro and R. Moliner, Carbonaceous materials as catalysts for decomposition of methane, *Chem. Eng. J*., **140**, 432 (2008).

192. N. Shah, D. Panjala and G. P. Huffman, Hydrogen Production by Catalystic Decomposition of Methane, *Energy & Fuels*, **15**, 1528 (2001).
193. D. Torres, S. D. Llobet, J. L. Pinilla, M. J. La´zaro, I. Suelves and R. Moliner, Hydrogen production by catalytic decomposition of methane using a Fe-based catalyst in a fluidized bed reactor, *J. Nat. Gas Chem*., **21**, 367 (2012).
194. L. Jin, H. Si, J. Zhang, P. Lin, Z. Hu, B. Qiu and H. Hu, Preparation of activated carbon supported Fe/Al_2O_3 catalyst and its application for hydrogen production by catalytic methane decomposition, *Int. J. Hydrogen Energy*, **38**, 10373 (2013).
195. T. V. Reshetenko, L. B. Avdeeva, V. A. Ushakov, E. M. Moroz, A. N. Shmakov, V. V. Kriventsov, D. I. Kochubey, Yu. T. Pavlyukhin, A. L. Chuvilin and Z. R. Ismagilov, Coprecipitated iron-containing catalysts (Fe-Al_2O_3, Fe-Co- Al_2O_3, Fe-Ni- Al_2O_3) for methane decomposition at moderate temperatures Part II. Evolution of the catalysts in reaction, *Appl. Catal. A: Gen.*, **270**, 87 (2004).
196. S. Takenaka, M. Serizawa and K. Otsuka, Formation of filamentous carbons over supported Fe catalysts through methane decomposition, *J. Catal.*, **222**, 520 (2004).
197. A. Konieczny, K. Mondal, T.Wiltowski and P. Dydo, Catalyst development for thermocatalytic decomposition of methane to hydrogen, *Int. J. Hydrogen Energy*, **33**, 264 (2008).
198. M. A. Ermakova, D. Y. Ermakov, A. L. Chuvilin and G. G. Kuvshinov, Effect of Sn on methane decomposition over Fe supported catalysts to produce carbon, *J. Catal.*, **201**, 183 (2001).
199. P. F. Oliveira, L. P. Ribeiro, M.G. Rosmaninho, J. D. Ardisson, A. Dias and R. M. Lago, Effect of Sn on methane decomposition over Fe supported catalysts to produce carbon, *Hyperfine. Interact.*, **203**, 67 (2011).
200. D. Yamaguchi, L. Tang, L. Wong, N. Burke, D. T. K. Nguyen and K. Chiang, Hydrogen production through methane steam cyclic redox processes with iron-based metal oxides, *Int. J. Hydrogen Energy*, **36**, 6646 (2011).
201. J. L. Pinilla, D. Torres, M. J. La´zaro, I. Suelves, R. Moliner, I. Can˜adas, J. Rodrı´guez, A. Vidal and D. Martı´nez, Metallic and carbonaceous - based catalysts performance in the solar catalytic decomposition of methane for hydrogen and carbon production, *Int. J. Hydrogen Energy*, **37**, 9645 (2012).